An effective strong-coupling theory of composite particles in UV-domain

She-Sheng Xue

ICRANet,
Piazzale della Repubblica 10, 10-65122, Pescara, Italy
Physics Department, Sapienza University of Rome,
Piazzale Aldo Moro 5, 00185 Roma, Italy

E-mail: xue@icra.it

ABSTRACT: We briefly review the effective field theory of massive composite particles, their gauge couplings and characteristic energy scale in the UV-domain of UV-stable fixed point of strong four-fermion coupling, then mainly focus the discussions on the decay channels of composite particles into the final states of the SM gauge bosons, leptons and quarks. We calculate the rates of composite bosons decaying into two gauge bosons $\gamma\gamma$, γZ^0, W^+W^-, Z^0Z^0 and give the ratios of decay rates of different channels depending on gauge couplings only. It is shown that a composite fermion decays into an elementary fermion and a composite boson, the latter being an intermediate state decays into two gauge bosons, leading to a peculiar kinematics of final states of a quark (or a lepton) and two gauge bosons. These provide experimental implications of such an effective theory of composite particles beyond the SM. We also present some speculative discussions on the channels of composite fermions decaying into WW, WZ and ZZ two boson-tagged jets with quark jets, or to four-quark jets. Moreover, at the same energy scale of composite particles produced in high-energy experiments, composite particles are also produced by high-energy sterile neutrino (dark matter) collisions, their decays lead to excesses of cosmic ray particles in space and signals of SM particles in underground laboratories.

Contents

1 Introduction

The parity-violating (chiral) gauge symmetries and spontaneous/explicit breaking of these symmetries for the hierarchy of fermion masses have been at the center of a conceptual elaboration that has played a major role in donating to mankind the beauty of the SM for particle physics. The Nambu-Jona-Lasinio (NJL) model [1] of dimension-6 four-fermion operators at high energies and its effective counterpart, the phenomenological model [2–7] of the elementary Higgs boson and its Yukawa-coupling to fermions at low energies, provide an elegant and simple description for the electroweak symmetry breaking and intermediate gauge boson masses. After a great experimental effort for many years, using data recorded at $\sqrt{s} = 7, 8\,\mathrm{TeV}$ experiments of pp collision at the Large Hadron Collider (LHC), the ATLAS [8] and CMS [9] collaborations have shown the first observations of a $125\,\mathrm{GeV}$ scalar particle in the search for the SM Higgs boson. This far-reaching result begins to shed light on this most elusive and fascinating arena of fundamental particle physics. Recently, in the Run-2 of the upgraded LHC, the preliminary results on $\sqrt{s} = 13\,\mathrm{TeV}$ pp collision data are prepared by ATLAS [10] and CMS [11] to search for new (beyond the SM) resonant and/or nonresonant phenomena that might manifest themselves in the high-energy regime with final states of diboson, dilepton, dijet and so forth. The diphoton channel preliminarily showed the trace of a new resonance at the diphoton invariant mass $\mathcal{M}_{\gamma\gamma}$, which however has not been further confirmed by increasing the integrated luminosity and energy of pp collisions.

1.1 Weak-interacting four-fermion operators and symmetry-breaking phase

The dynamics of new physics at high energies may be represented by an effective theory of high-dimensional operators of fermion fields, e.g., dimension-6 four-fermion operators, preserving at least the SM gauge symmetries. The strong technicolor dynamics of extended gauge theories at the TeV scale was invoked [22–27] to have a natural scheme incorporating the relevant four-fermion operator $G(\bar{\psi}_L^{ia} t_{Ra})(\bar{t}_R^b \psi_{Lib})$ of the $\langle \bar{t}t \rangle$-condensate model [28], to generate the top-quark mass via spontaneous symmetry breaking (SSB). On the other hand, these relevant operators can be constructed on the basis of phenomenology of the SM at low-energies. In 1989, several authors [28–33] suggested that the SM symmetry breakdown could be a dynamical mechanism of the NJL type that intimately involves the top quark at the high-energy scale Λ. Since then, many models based on this idea have been studied [34, 35]. In the scenes of renormalization group (scaling) invariance and resultant renormalization-group (RG) equations, there is a scaling region (IR-domain) of the infrared (IR) stable fixed point of four-fermion operators, the low-energy SM physics was supposed to be achieved by the RG equations in the IR-domain with the electroweak scale $v \approx 239.5\,\text{GeV}$ [25–28, 33]. It is in this IR-domain, we recently present the detailed study of hierarchy mass spectrum of SM fermions: from top quark to electron neutrino [12, 13], on the basis of effective four-fermion operators of Einstein-Cartan type, as will be shown in section 2.

1.2 Strong-interacting four-fermion operators and gauge-symmetric phase

In addition to the IR-domain of weak-coupling four-fermion operators in the SSB phase where the low-energy SM is realized, we find a scaling region (UV-domain) of the ultraviolet (UV) stable fixed point of strong-coupling four-fermion operators in the gauge-symmetric phase. In this UV-domain at high energies, it realizes an effective theory of composite bosons and fermions composed by SM elementary fermions, these composite particles and their interactions preserving the SM gauge symmetries [14–20]. This is the issue that we would like to focus in this article.

In refs. [20, 21], we have already presented discussions on the possible decay channels of composite bosons and fermions into final states of jets and leptons in the framework of effective four-fermion operators in high energies. In this article, we focus on the discussions on the possible channels of composite bosons decaying into two SM gauge bosons, and composite fermions decaying into two SM gauge bosons (diboson) and a quark/lepton, as well as their experimental implications. It is preliminarily shown that the diphoton channel of composite bosons decay should have the largest branching ratio, however other diboson channels should also contribute to the invariant mass $\mathcal{M}$ of possible composite-boson resonance. Instead, composite fermions decay into a composite boson and a quark/lepton, the former is an intermediate state, which then decays into two bosons, i.e., a quark-diboson or lepton-diboson channel. These final states and their kinematic relations of such a quark-diboson or lepton-diboson channel are peculiar. This provides a possibility/criterion to verify the effective theory of composite particles in high-energy experiments.

1.3 Article arrangement

In section 2, we present the SM gauge-symmetric operators of four-fermion interactions of Einstein-Cardan type and the brief discussion of their possible origin. Some explanations and clarifications of the low-energy IR-domain for the SM and the high-energy UV-domain for an effective field theory of composite particles are given in section 3. After showing the composite particle spectrum and effective Lagrangian in sections 4 in the framework of SM fermion content and gauge symmetries, we discuss in sections 5 and 6.1 the main results that the composite boson and fermion decay into SM gauge bosons and/or elementary fermions in connection with high-energy experiments. In the final section, we present some discussions and speculations on the possible channels of composite particles interacting with SM particles, that could be relevant to some experiments at the energy scale of composite particles.

2 Four-fermion operators beyond the SM

In order for a self-contained and self-consistent article, as well as for readers' convenience, we include this section of describing effective four-fermion operators at the cutoff Λ that was similarly presented in ref. [13] for discussing the hierarchy spectrum of SM fermions in the IR-domain. It is also necessary to present these effective four-fermion operators at the cutoff Λ to clarify its induced Lagrangian of the composite particle spectra and interactions in the UV-domain.

2.1 Regularization and quantum gravity

Up to now the theoretical and experimental studies tell us the chiral gauge-field interactions to fermions in the lepton-quark family that is replicated three times and mixed. The spontaneous breaking of these chiral gauge symmetries and generating of fermion masses are made by the Higgs field sector. In the IR-fixed-point domain of weak four-fermion coupling or equivalently weak Yukawa coupling, the SM Lagrangian with all relevant operators (parametrizations) is realized and behaves an effective and renormalizable field theory in low energies. To achieve these SM relevant operators, a finite field theory of chiral-gauge interactions should be well-defined by including the quantum gravity that naturally provides a space-time regularization (UV cutoff). As an example, the finite superstring theory is proposed by postulating that instead of a simple space-time point, the fundamental space-time "constituents" is a space-time "string". The Planck scale is a plausible cut-off, at which all principle and symmetries are fully respected by gauge fields and particle spectra, fermions and bosons.

In this article, we do not discuss how a fundamental theory at the Planck scale induces high-dimensional operators. Instead, as a postulation or motivation, we argue the presence of at least four-fermion operators beyond the SM from the following point view. A well-defined quantum field theory for the SM Lagrangian requires a natural regularization (UV cutoff Λ) fully preserving the SM chiral-gauge symmetry. The quantum gravity naturally provides a such regularization of discrete space-time with the minimal length $\tilde{a} \approx$

1.2 $a_{\rm pl}$ [36–39], where the Planck length $a_{\rm pl} \sim 10^{-33}$ cm and scale $\Lambda_{\rm pl} = \pi/a_{\rm pl} \sim 10^{19}$ GeV. However, the no-go theorem [40–42] tells us that there is no any consistent way to regularize the SM bilinear fermion Lagrangian to exactly preserve the SM chiral-gauge symmetries, which must be explicitly broken at the scale of fundamental space-time cutoff $\tilde{a}$. This implies that the natural quantum-gravity regularization for the SM should lead us to consider at least dimension-6 four-fermion operators originated from quantum gravity effects at short distances.[1] As a model, we adopt the four-fermion operators of the torsion-free Einstein-Cartan Lagrangian within the framework of the SM fermion content and gauge symmetries. We stress that a fundamental theory at the UV cutoff is still unknown.

2.2 Einstein-Cartan theory with SM gauge symmetries and fermion content

The Lagrangian of torsion-free Einstein-Cartan (EC) theory reads,

$$\mathcal{L}_{EC}(e,\omega,\psi) = \mathcal{L}_{EC}(e,\omega) + \bar{\psi}e^\mu \mathcal{D}_\mu \psi + G J^d J_d, \tag{2.1}$$

where the gravitational Lagrangian $\mathcal{L}_{EC} = \mathcal{L}_{EC}(e,\omega)$, tetrad field $e_\mu(x) = e_\mu{}^a(x)\gamma_a$, spin-connection field $\omega_\mu(x) = \omega_\mu^{ab}(x)\sigma_{ab}$, the covariant derivative $\mathcal{D}_\mu = \partial_\mu - ig\omega_\mu$ and the axial current $J^d = \bar{\psi}\gamma^d\gamma^5\psi$ of massless fermion fields. The four-fermion coupling G relates to the gravitation-fermion gauge coupling g and fundamental space-time cutoff $\tilde{a}$.

In the context of the SM one-family fermion content and gauge symmetries, we consider massless, two-component, left- and right-handed Weyl fermions ψ_L^f (doublets) and ψ_R^f (singlets) carrying the quantum numbers of the SM $SU_L(2) \times U_Y(1)$ chiral gauge symmetries, where "f" is the fermion-family index, as well as three right-handed Weyl sterile neutrinos ν_R^f and their left-handed conjugated fields $\nu_R^{fc} = i\gamma_2(\nu_R)^*$, which do not carry any quantum number of SM gauge symmetries. Analogously to the EC theory (2.1), we obtain a torsion-free, diffeomorphism and *local* gauge-invariant Lagrangian

$$\begin{aligned}
\mathcal{L} = \mathcal{L}_{EC}(e,\omega) &+ \sum_f \bar{\psi}_{L,R}^f e^\mu \mathcal{D}_\mu \psi_{L,R}^f + \sum_f \bar{\nu}_R^{fc} e^\mu \mathcal{D}_\mu \nu_R^{fc} \\
&+ G \left(J_L^\mu J_{L,\mu} + J_R^\mu J_{R,\mu} + 2J_L^\mu J_{R,\mu} \right) \\
&+ G \left(j_L^\mu j_{L,\mu} + 2J_L^\mu j_{L,\mu} + 2J_R^\mu j_{L,\mu} \right),
\end{aligned} \tag{2.2}$$

where the SM gauge fields A_μ are present in the co-variant derivative $\mathcal{D}_\mu$ to preserve the SM gauge symmetries, and axial currents read

$$J_{L,R}^\mu \equiv \sum_f \bar{\psi}_{L,R}^f \gamma^\mu \gamma^5 \psi_{L,R}^f, \quad j_L^\mu \equiv \sum_f \bar{\nu}_R^{fc} \gamma^\mu \gamma^5 \nu_R^{fc}. \tag{2.3}$$

The four-fermion coupling G is unique for all four-fermion operators and high-dimensional fermion operators ($d > 6$) are neglected.

---

[1] In the regularized and quantized EC theory [36–39] with a basic space-time cutoff, in addition to dimension-6 four-fermion operators, there are high-dimensional fermion operators ($d > 6$), e.g., $\partial_\sigma J^\mu \partial^\sigma J_\mu$, which are suppressed at least by $\mathcal{O}(\tilde{a}^4)$.

By using the Fierz theorem [43, 44], the dimension-6 four-fermion operators in eq. (2.2) can be written as [21]

$$+ (G/2) \left(J_L^\mu J_{L,\mu} + J_R^\mu J_{R,\mu} + j_L^\mu j_{L,\mu} + 2 J_L^\mu j_{L,\mu} \right) \tag{2.4}$$

$$- G \sum_{ff'} \left(\bar{\psi}_L^f \psi_R^{f'} \bar{\psi}_R^{f'} \psi_L^f + \bar{\nu}_R^{fc} \psi_R^{f'} \bar{\psi}_R^{f'} \nu_R^{fc} \right), \tag{2.5}$$

which preserve the SM gauge symmetries. Equations (2.4) and (2.5) represent repulsive and attractive operators respectively. The former (2.4) are suppressed by the cutoff $\mathcal{O}(\Lambda^{-2})$, and cannot become relevant and renormalizable operators of effective dimension-4. Thus the torsion-free EC theory with the attractive four-fermion operators reads,

$$\mathcal{L} = \mathcal{L}_{EC} + \sum_f \bar{\psi}_{L,R}^f e^\mu \mathcal{D}_\mu \psi_{L,R}^f + \sum_f \bar{\nu}_R^{fc} e^\mu \mathcal{D}_\mu \nu_R^{fc}$$
$$- G \sum_{ff'} \left(\bar{\psi}_L^f \psi_R^{f'} \bar{\psi}_R^{f'} \psi_L^f + \bar{\nu}_R^{fc} \psi_R^{f'} \bar{\psi}_R^{f'} \nu_R^{fc} \right) + \text{h.c.}, \tag{2.6}$$

where the two component Weyl fermions ψ_L^f and ψ_R^f respectively are the $SU_L(2) \times U_Y(1)$ gauged doublets and singlets of the SM. For the sake of compact notations, ψ_R^f are also used to represent ν_R^f, which have no any SM quantum numbers. All fermions are massless, they are four-component Dirac fermions $\psi^f = (\psi_L^f + \psi_R^f)$, two-component left-handed Weyl neutrinos ν_L^f and four-component sterile Majorana neutrinos $\nu_M^f = (\nu_R^{fc} + \nu_R^f)$ whose kinetic terms read

$$\bar{\nu}_L^f e^\mu \mathcal{D}_\mu \nu_L^f, \quad \bar{\nu}_M^f e^\mu \mathcal{D}_\mu \nu_M^f = \bar{\nu}_R^f e^\mu \mathcal{D}_\mu \nu_R^f + \bar{\nu}_R^{fc} e^\mu \mathcal{D}_\mu \nu_R^{fc}. \tag{2.7}$$

In eq. (2.6), f and f' ($f, f' = 1, 2, 3$) are fermion-family indexes summed over respectively for three lepton families (charge $q = 0, -1$) and three quark families ($q = 2/3, -1/3$). Equation (2.6) preserves not only the SM gauge symmetries and global fermion-family symmetries, but also the global symmetries for fermion-number conservations. We adopt the effective four-fermion operators (2.6) in the context of a well-defined quantum field theory at the high-energy scale Λ.

2.3 Fermion-family symmetry and mass eigenstate

As argued in the introduction section 2.1, the origin of effective four-fermion operators in eqs. (2.1)–(2.6) is due to the quantum gravity that couples to all fermion fields and provides a natural regularization for chiral gauge field theories, like the SM, at the UV cutoff Λ. Therefore, there is no any reason to assume different four-fermion coupling G's for different fermions that equally couple to the gravitational field in the torson-free Einstein-Cartan theory (2.1).

It should be further clarified that in the effective Lagrangian (2.6) at the cutoff Λ, (i) the massless SM fermion fields are interacting *gauge eigenstates* of the SM gauge symmetries $SU_c(3) \times SU_L(2) \times U_Y(1)$; (ii) due to the unique four-fermion coupling G, there are exact global fermion-family $U_L(3) \times U_R(3)$ chiral symmetries, i.e., flavor or horizon symmetries with respect to different charges $q = 0, -1, 2/3, -1/3$ of fermions in different families.

In order to study the gauge-boson-fermion and four-fermion interactions in terms of fermion mass-energy spectra and currents, measured as physical final states, we adopt the energy-*mass eigenstates* of fermions in the following discussions of entire article. The unitary chiral transformations $\mathcal{U}_L \in U_L(3)$ and $\mathcal{U}_R \in U_R(3)$, where $\mathcal{U}_L$ and $\mathcal{U}_R$ are related by a unitary matrix $\mathcal{V}$, can be performed from gauge eigenstates to mass eigenstates (up- and down-quark sectors as example):

$$\psi_L^u \to \mathcal{U}_L^u \, \psi_L^u, \quad \psi_R^u \to \mathcal{U}_R^u \, \psi_R^u; \quad \mathcal{U}_{L,R}^u \in U_{L,R}^u(3), \tag{2.8}$$

and

$$\psi_L^d \to \mathcal{U}_L^d \, \psi_L^d, \quad \psi_R^d \to \mathcal{U}_R^d \, \psi_R^d; \quad \mathcal{U}_{L,R}^d \in U_{L,R}^d(3), \tag{2.9}$$

so that in eq. (2.6) the fermion-family indexes $f = f'$, i.e., $\delta_{ff'}$ respectively for the u-quark sector and the d-quark sector. As a result, all quark fields are mass eigenstates, the four-fermion operators (2.6) are "diagonal" only for each quark family without fermion-family mixing,

$$- G \sum_{f=1,2,3} \left[\bar{\psi}_L^f \psi_R^f \bar{\psi}_R^f \psi_L^f \right]_{2/3}^{\text{up}} - G \sum_{f=1,2,3} \left[\bar{\psi}_L^f \psi_R^f \bar{\psi}_R^f \psi_L^f \right]_{-1/3}^{\text{down}}. \tag{2.10}$$

In the following, we adopt this representation and our notations will be only for the first SM family, however, they are the same for the second and third families.

In this representation, bilinear fermion-mass operators $\langle \psi_R^f \bar{\psi}_L^f \rangle + \text{h.c.}$, i.e., quark-mass matrices are diagonalized in the fermion-family space by the biunitary transformations

$$M^u \Rightarrow M_{\text{diag}}^u = (m_1^u, m_2^c, m_3^t) = \mathcal{U}_L^{u\dagger} M^u \mathcal{U}_R^u, \tag{2.11}$$

$$M^d \Rightarrow M_{\text{diag}}^d = (m_1^d, m_2^s, m_3^b) = \mathcal{U}_L^{d\dagger} M^d \mathcal{U}_R^d, \tag{2.12}$$

where all quark masses (eigenvalues) are positive, $\mathcal{U}_L$ and $\mathcal{U}_R$ are related by

$$\mathcal{U}_L^{u,d} = \mathcal{V}^{u,d} \mathcal{U}_R^{u,d}, \tag{2.13}$$

and $\mathcal{V}^{u,d}$ is a unitary matrix, see for example [45, 46]. Using unitary matrices $\mathcal{U}_{L,R}^u$ (2.8) and $\mathcal{U}_{L,R}^d$ (2.9), up to a diagonal phase matrix we define the unitary quark-family mixing matrices,

$$\begin{aligned} \mathcal{U}_L^{u\dagger} \mathcal{U}_L^d, & \quad \mathcal{U}_L^{u\dagger} \mathcal{U}_R^d, \\ \mathcal{U}_R^{u\dagger} \mathcal{U}_L^d, & \quad \mathcal{U}_R^{u\dagger} \mathcal{U}_R^d. \end{aligned} \tag{2.14}$$

where the first element is the CKM matrix $U = U_L^q \equiv \mathcal{U}_L^{u\dagger} \mathcal{U}_L^d$. The similar discussions for the lepton sector can be found in ref. [13].

In the IR effective theory in the IR-domain, the nonzero and different expectational values of fermion-mass operators $\langle \psi_R^f \bar{\psi}_L^f \rangle \propto m^f \neq 0$ (2.11) and fermion-family hierarchy $m^f \neq m^{f'}$ can be developed due to both spontaneous-symmetry and explicit-symmetry breaking of chiral symmetries [12]. In this case, apart from the breaking of the SM chiral gauge symmetries, fermion-family (flavor) $U_L(3) \times U_R(3)$ symmetries are broken to the

U(1) symmetry for each fermion family, i.e., $U_1(1) \times U_2(1) \times U_3(1)$ for the four-fermion operators (2.10), two-fermion operators (2.11) and (2.12). However, the mass eigenstates of the SM *elementary* fermions are different from their chiral-gauge eigenstates, i.e., the interaction vertexes of the chiral-gauge-boson $W^\pm$ and massive fermions are not diagonal in the fermion-family space based on the mass eigenstates of fermions, as can be seen in the kinetic terms of the effective Lagrangian (2.6).

In the UV effective theory in the UV-domain, instead, the chiral and flavor symmetries are preserved for $m^f = 0$, indicating that gauge and mass eigenstates of *composite* particles are the same. In sections 3.1.3 and 4.2.3, we will come back to the discussions of the flavor-changing-neutral-current (FCNC) processes, considering the chiral- and flavor-symmetries breaking (preserving) of IR (UV) effective theory in the IR (UV) domain respectively.

2.4 SM gauge-symmetric four-fermion operators

Using eq. (2.10) and we explicitly show SM gauge symmetric four-fermion operators. In the quark sector, the four-fermion operators are

$$G\left[\left(\bar{\psi}_L^{ia} t_{Ra}\right)\left(\bar{t}_R^b \psi_{Lib}\right) + \left(\bar{\psi}_L^{ia} b_{Ra}\right)\left(\bar{b}_R^b \psi_{Lib}\right)\right] + \text{``terms''}, \tag{2.15}$$

where a, b and i, j are the color and flavor indexes of the top and bottom quarks, the quark $SU_L(2)$ doublet $\psi_L^{ia} = (t_L^a, b_L^a)$ and singlet $\psi_R^a = t_R^a, b_R^a$ are the eigenstates of electroweak interaction. The first and second terms in eq. (2.15) are respectively the four-fermion operators of top-quark channel [28] and bottom-quark channel, whereas "terms" stands for the first and second quark families that can be obtained by substituting $t \to u, c$ and $b \to d, s$ [20, 50, 51].

In the lepton sector with three right-handed sterile neutrinos ν_R^ℓ ($\ell = e, \mu, \tau$), the four-fermion operators in terms of gauge eigenstates are,

$$G\left[\left(\bar{\ell}_L^i \ell_R\right)\left(\bar{\ell}_R \ell_{Li}\right) + \left(\bar{\ell}_L^i \nu_R^\ell\right)\left(\bar{\nu}_R^\ell \ell_{Li}\right) + \left(\bar{\nu}_R^{\ell c} \nu_R^\ell\right)\left(\bar{\nu}_R^\ell \nu_R^{\ell c}\right)\right], \tag{2.16}$$

preserving all SM gauge symmetries, where the lepton $SU_L(2)$ doublets $\ell_L^i = (\nu_L^\ell, \ell_L)$, singlets ℓ_R and the conjugate fields of sterile neutrinos $\nu_R^{\ell c} = i\gamma_2(\nu_R^\ell)^*$. Coming from the second term in eq. (2.6), the last term in eq. (2.16) preserves the symmetry $U_{\text{lepton}}(1)$ for the lepton-number conservation, although $(\bar{\nu}_R^\ell \nu_R^{\ell c})$ violates the lepton number of family "ℓ" by two units.

Similarly, from the second term in eq. (2.6) there are following four-fermion operators

$$G\left[\left(\bar{\nu}_R^{\ell c} \ell_R\right)\left(\bar{\ell}_R \nu_R^{\ell c}\right) + \left(\bar{\nu}_R^{\ell c} u_{a,R}^\ell\right)\left(\bar{u}_{a,R}^\ell \nu_R^{\ell c}\right) + \left(\bar{\nu}_R^{\ell c} d_{a,R}^\ell\right)\left(\bar{d}_{a,R}^\ell \nu_R^{\ell c}\right)\right], \tag{2.17}$$

where quark fields $u_{a,R}^\ell = (u, c, t)_{a,R}$ and $d_{a,R}^\ell = (d, s, b)_{a,R}$.

2.5 Four-fermion operators of quark-lepton interactions

Although the four-fermion operators in eq. (2.6) do not have quark-lepton interactions, we consider the following SM gauge-symmetric four-fermion operators that contain quark-lepton interactions [12, 13, 47],

$$G\left[\left(\bar{\ell}_L^i e_R\right)\left(\bar{d}_R^a \psi_{Lia}\right) + \left(\bar{\ell}_L^i \nu_R^e\right)\left(\bar{u}_R^a \psi_{Lia}\right)\right] + (\cdots), \tag{2.18}$$

where $\ell_L^i = (\nu_L^e, e_L)$ and $\psi_{Lia} = (u_{La}, d_{La})$ for the first family. The $(\cdots)$ represents for the second and third families with substitutions: $e \to \mu, \tau$, $\nu^e \to \nu^\mu, \nu^\tau$, and $u \to c, t$ and $d \to s, b$. The four-fermion operators (2.18) of quark-lepton interactions are not included in eq. (2.6), since leptons and quarks are in separated representations of SM gauge groups. They should be expected in the framework of Einstein-Cartan theory and SO(10) unification theory [48, 49].

3 IR-stable and UV-stable fixed points and their scaling regions

Apart from what is possible new physics at the UV scale Λ explaining the origin of these effective four-fermion operators, it is essential and necessary to study: (i) the phase diagram in the space of these effective four-fermion operator couplings; (ii) which dynamics of these operators undergo in terms of their couplings as functions of running energy scale μ; (iii) associating to these dynamics where infrared (IR) and/or ultraviolet (UV) stable fixed point of physical couplings locates; (iv) in the IR and/or UV domains (scaling regions) of these stable fixed points, which operators become physically relevant and renormalizable following RG equations (scaling laws), and other irrelevant operators are suppressed by the cutoff at least $\mathcal{O}(\Lambda^{-2})$.

3.1 Symmetry-breaking phase and the IR-domain of the IR-stable fixed point

In the NJL symmetry-breaking phase of weak coupling $G > G_c$,[2] where G_c is the weak critical coupling of the NJL dynamics, the low-energy SM physics was supposed to be achieved in the IR-domain ($G \gtrsim G_c$) of IR-stable fixed point [25–28, 33]. Bardeen, Hill and Lindner (BHL) proposed the effective Lagrangian of the $t\bar{t}$-condensate model [28],

$$L = L_{\text{kinetic}} + g_{t0}(\bar{\psi}_L t_R H + \text{h.c.}) + \Delta L_{\text{gauge}}$$
$$+ Z_H |D_\mu H|^2 - m_{0H}^2 H^\dagger H - \frac{\lambda_0}{2}(H^\dagger H)^2, \tag{3.1}$$

with a massive composite Higgs boson $H = (\bar{t}t)$ and massless Goldstone bosons $(\bar{t}\gamma_5 t)$ and $(\bar{t}\gamma_5 b)$, which are the longitudinal modes of massive intermediate gauge bosons. The composite Higgs' bare form-factor (wave-function renormalization) Z_H and masss m_{0H}, as well as its Yukawa g_{t0} and quartic λ_0 couplings are defined at an intermediate scale $\mathcal{E}$ ($v < \mathcal{E} < \Lambda$), that will be clear below (3.12). Renormalized quantities, like Yukawa coupling $\bar{g}_t(\mu^2)$ and quartic couplings $\bar{\lambda}(\mu^2)$ are defined at the running energy scale μ and satisfy the RG equations in the IR-domain,

$$16\pi^2 \frac{d\bar{g}_t}{dt} = \left(\frac{9}{2}\bar{g}_t^2 - 8\bar{g}_3^2 - \frac{9}{4}\bar{g}_2^2 - \frac{17}{12}\bar{g}_1^2\right)\bar{g}_t, \tag{3.2}$$

$$16\pi^2 \frac{d\bar{\lambda}}{dt} = 12\left[\bar{\lambda}^2 + (\bar{g}_t^2 - A)\bar{\lambda} + B - \bar{g}_t^4\right], \quad t = \ln\mu \tag{3.3}$$

---

[2]In the symmetric phase of extremal weak coupling $G < G_c$, all four-fermion interacting amplitudes are suppressed by the cutoff Λ.
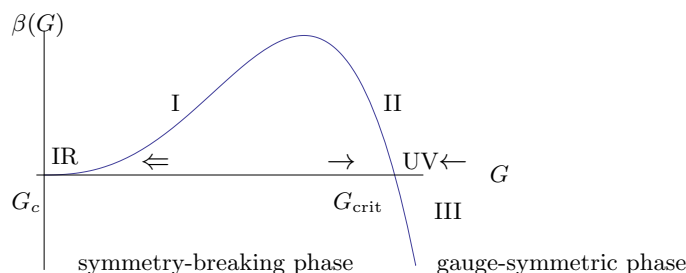
Figure 1. This is a sketch [20] to qualitatively show the behavior of the β-function in terms of the four-fermion coupling G. We indicate the IR-stable fixed point G_c and a possible UV-stable fixed point $G_{\rm crit}$, the latter separates the symmetry-breaking phase (positive $\beta(G)$-function) from the gauge-symmetric phase (negative $\beta(G)$-function). We also indicate the different parts of $\beta(G)$-function: the positively increasing part "I" and the IR-domain where RG flow approaches (thick left arrow) to the IR-fixed point, as energy scale μ decreases; (ii) the positively decreasing part "II" and the negative part "III", as well as the UV-domain where RG flow approaches (thin right and left arrows) to the UV-fixed point, as the running energy scale μ increases.

where one can find A, B and RG equations for running gauge couplings $g_{1,2,3}^2$ in eqs. (4.7), (4.8) of ref. [28].

This IR-domain of IR-stable fixed point G_c can be illustrated by a positive $\beta(G)$-function for $G \gtrsim G_c$. Taking into account one fermion-loop contribution (tadpole diagram) from the SSB-relevant top-quark channel (2.15), we calculate the gap equation for top-quark mass $m_t \neq 0$, and obtain the β-function

$$\beta(G) \equiv \mu \frac{dG}{d\mu} \approx 2\frac{G^2}{G_c}\left(\frac{\mu}{\mathcal{E}}\right)^2\left[1 + \ln\left(\frac{\mathcal{E}}{\mu}\right)^2\right] > 0, \tag{3.4}$$

for $G \gtrsim G_c \equiv 8\pi^2/(N_c\mathcal{E}^2)$ and intermediate energy scale $\mathcal{E} > \mu \gtrsim v$, where $N_c = 3$ is the number of colors. The positive β-function of eq. (3.4) indicates that an IR-stable fixed point G_c and the IR-domain $G \to G_c + 0^+$ as the running energy scale $\mu \to v$, as shown the part "I" of the $\beta(G)$-function in figure 1. As the energy scale μ decreases, indicated by a thick arrow in figure 1, the RG flow is attracted to the IR-stable fixed point, and the effective SM of particle physics in low energies is realized in this IR-domain (vicinity) of IR-stable fixed point.

3.1.1 Resolution to the $t\bar{t}$-condensate model

Both experimental m_t and m_H values of top-quark and Higgs-boson masses were unknown in the early 1990s. In order to find low-energy values m_t and m_H close to the IR-stable fixed point, BHL [28] imposed the compositeness conditions $\tilde{Z}_H(\mu) = 1/\bar{g}_t^2(\mu) \to 0$ and $\tilde{\lambda} = \bar{\lambda}(\mu)/\bar{g}_t^4(\mu) \to 0$, as energy scale $\mu \to \Lambda$ for different values of the high-energy cutoff Λ as the boundary conditions to solve the RG equations (3.2) and (3.3). As a result, masses m_t, m_H and Higgs-decay width obtained do not agree with experimental values, thus the BHL $t\bar{t}$-condensate model was firmly excluded. From the theoretical point of view, the compositeness conditions implies that the BHL composite Higgs boson is a *loosely* bound
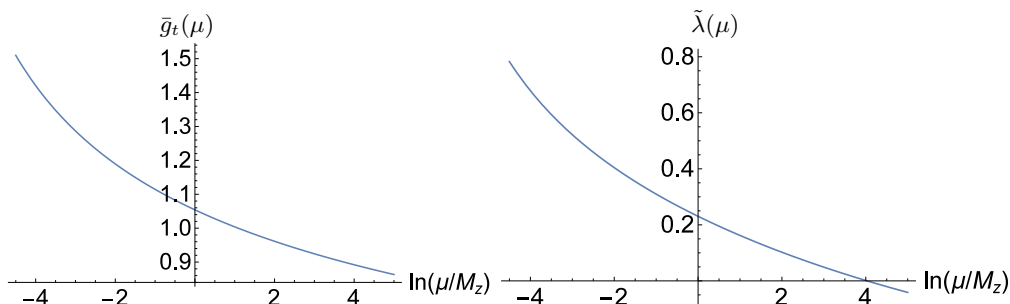
Figure 2. Using experimentally measured SM quantities (including m_t and m_H) as boundary values, we uniquely solve the RG equations for the composite Higgs-boson model [28], we find [20, 51] the effective top-quark Yukawa coupling $\bar{g}_t(\mu)$ (left) and effective Higgs quartic coupling $\tilde{\lambda}(\mu)$ (right) in the range $1.0\,\mathrm{GeV} \lesssim \mu \lesssim 13.5\,\mathrm{TeV}$. Note that $\tilde{\lambda}(\mathcal{E}) = 0$ at $\mathcal{E} \approx 5.14\,\mathrm{TeV}$ and $\tilde{\lambda}(\mu) < 0$ for $\mu > \mathcal{E}$.

state of top and anti-top-quark pair ($\bar{t}t$) because its wave-function renormalization $\tilde{Z}_H(\mu)$ goes to zero as $\mu \to \Lambda$.

Instead, we adopted [20, 51] the experimental values of the top-quark and Higgs-boson masses,

$$m_H = 126 \pm 0.5\,\mathrm{GeV}; \quad m_t = 172.9 \pm 0.8\,\mathrm{GeV}, \tag{3.5}$$

and used the mass-shell conditions $m_t = \bar{g}_t(m_t)v/\sqrt{2}$ and $m_H^2/2 = \tilde{\lambda}(m_H)v^2$, as infrared boundary conditions to integrate the RG equations (3.2) and (3.3) so as to uniquely determine the functions of top-quark Yukawa $\bar{g}_t(\mu)$ and Higgs-quartic $\tilde{\lambda}(\mu)$ couplings (see figure 2), as well as to obtain the finite values $\tilde{Z}_H(\mathcal{E}) \approx 1.26$ and the intermediate energy scale $\mathcal{E} \approx 5.1\,\mathrm{TeV}$ for $\tilde{\lambda}(\mathcal{E}) = 0$. Our results (figure 2) are radically different from the BHL results,[3] not only the completely different behaviors and numerical values of the Yukawa $\bar{g}_t(\mu)$ and quartic $\tilde{\lambda}(\mu)$ couplings that will be discussed in next subsection 3.1.2, but also (i) the composite Higgs boson is a *tightly* bound state of $\bar{t}t$ pair for finite values $\tilde{Z}_H(\mu)$, as if it is *an elementary* Higgs boson; (ii) the phase transition from the symmetry-breaking phase to the symmetric phase is indicated by $\tilde{\lambda}(\mu) \to 0^+$ as $\mu \to \mathcal{E} + 0^-$, will be discussed in section 3.3.1; (iii) the drastically fine-tuning (hierarchy) problem can be resolved, since the intermediate scale $\mathcal{E}$ ($v < \mathcal{E} \ll \Lambda$) replaces the high-energy cutoff Λ and sets into eq. (3.4), the gap-equation

$$\frac{1}{G_c} - \frac{1}{G} = \frac{1}{G_c}\left(\frac{m_t}{\mathcal{E}}\right)^2 \ln\left(\frac{\mathcal{E}}{m_t}\right)^2 > 0, \tag{3.6}$$

giving rise to a soft chiral-symmetry breaking scale $m_t \lesssim v$ and the pseudoscalar decay constant,

$$f_\pi^2 \approx \frac{N_c}{32\pi^2}m_t^2 \ln\frac{\mathcal{E}^2}{m_t^2} = \frac{N_c}{32\pi^2}\mathcal{E}^2\left(1 - \frac{G_c}{G}\right), \tag{3.7}$$

for more detailed discussions, see ref. [51].

In the IR-domain ($G \gtrsim G_c$) of unique four-fermion coupling G, it seems that the four-fermion operators (2.15) undergo the SSB, leading to the fermion-condensation $M_{ff'} =$

---

[3]Using the compositeness conditions $\tilde{Z}_H(\mu) = 1/\bar{g}_t^2(\mu) \to 0, \mu \to \Lambda$, we reproduced the BHL results: figures 4 and 5; tables I and II of ref. [28].

$-G\langle\bar{\psi}^f\psi^{f'}\rangle = m\delta_{ff'} \neq 0$, two diagonal mass matrices of quark sectors $q = 2/3$ and $q = -1/3$ satisfying $3 + 3$ mass-gap equations, see eqs. (2.11) and (2.12). It was demonstrated [50] that as an energetically favorable solution of the SSB ground state of the SM, only top-quark is massive ($m_t^{sb} = -G\langle\bar{\psi}_t\psi_t\rangle \neq 0$), otherwise in addition to those become the longitudinal modes of massive gauge bosons, there would be more Goldstone modes contributing the SSB-ground-state energy. In other words, among four-fermion operators (2.15) and (2.16), the $\langle\bar{t}t\rangle$-condensate model (3.1) is the unique channel undergoing the SSB of SM gauge symmetries, for the reason that this is energetically favorable, i.e., the ground-state energy is minimal when the maximal number of Goldstone modes are three and equal to the number of the longitudinal modes of massive gauge bosons in the SM. Moreover, the four-fermion operators (2.16) of the lepton sector do not undergo the SSB leading to the lepton-condensation $M_{ff'} = -G\langle\bar{\ell}^f\ell^{f'}\rangle = m_\ell\delta_{ff'} \neq 0$, i.e., two diagonal mass matrices of the lepton sector ($q = 0$ and $q = -1$). The reason is that the effective four-lepton coupling $(GN_c)/N_c$ is N_c-times smaller than the four-quark coupling (GN_c), where the color number $N_c = 3$. In the IR-domain ($G \gtrsim G_c$) of the IR-stable fixed point G_c, the effective four-quark coupling is above the critical value and the SSB occurs, whereas the effective four-lepton coupling is below the critical value and the SSB does not occur for the lepton sector.

As a result, only the top quark acquires its mass via the SSB and four-fermion operator (3.1) of the top-quark channel becomes the relevant operator following the RG equations in the IR domain [28]. While all other quarks and leptons do not acquire their masses via the SSB and their four-fermion operators (2.15), (2.16), (2.17), (2.18) are irrelevant dimension-6 operators, whose tree-level amplitudes of four-fermion scatterings are highly suppressed $\mathcal{O}[(\mu/\Lambda)^2]$, thus their deviations from the SM are nowadays experimentally inaccessible [21].

3.1.2 Experimental indications of tightly-bound composite Higgs boson?

The wave-function renormalization $\tilde{Z}_H(\mu) = 1/\bar{g}_t^2(\mu)$ represents the form-factor of composite Higgs boson. In the BHL case, the compositeness condition $\tilde{Z}_H(\mu) \to 0, \mu \to \Lambda$ is adapted, this implies that the BHL loosely-bound composite Higgs boson behaves very differently from the elementary Higgs boson, and significant deviations from the SM are expected. In theoretical calculations, the BHL Yukawa-coupling $\bar{g}_t^{BHL}(\mu)$ increases with energy μ, and Higgs-quartic coupling $\tilde{\lambda}^{BHL}(\mu)$ increases for $M_z < \mu \lesssim 5\,\text{TeV}$ (see figures 4 and 5 of ref. [28]), which are completely different from our results of figure 2. In experimental fact, the BHL results are firmly excluded by the measured values of Higgs mass and decay rate (width). Instead, in our case the non-vanishing $\tilde{Z}_H(\mu)$ means that after conventional wave-function and vertex renormalizations, the tightly-bound composite Higgs boson behaves as if an elementary particle. The deviations from the SM with an elementary Higgs boson are expected to be very small.

However, the effective top-Yukawa $\bar{g}_t(\mu)$ and Higgs-quartic $\tilde{\lambda}(\mu)$ couplings monotonically and slightly decrease as the energy scale μ increases over the range ($M_z < \mu < \mathcal{E}$), see figure 2. In the range $m_H < \mu < \mathcal{E}$, these might imply some effects on the rates or cross-sections of the following three dominate processes of Higgs-boson production and

decay [8, 9] or other relevant processes. Two-gluon fusion produces a Higgs boson via a top-quark loop, which is proportional to the effective Yukawa coupling $\bar{g}_t(\mu)$. Then, the produced Higgs boson decays into the two-photon state by coupling to a top-quark loop, and into the four-lepton state by coupling to two massive W-bosons or two massive Z-bosons. Due to the $\bar{t}t$-composite nature of Higgs boson, the one-particle-irreducible (1PI) vertexes of Higgs-boson coupling to a top-quark loop, to two massive W-bosons and to two massive Z-bosons are proportional to the effective Yukawa coupling $\bar{g}_t(\mu)$. As a result, both the Higgs-boson decaying rate $\Gamma_{H \to f}$ to each of these three channels and total decay rate $\Gamma_H^{\text{total}} = \sum_f \Gamma_{H \to f}$ are proportional to $\bar{g}_t^2(\mu)$, however the branching ratio $(\Gamma_{H \to f}/\Gamma_H^{\text{total}})$ of each Higgs-decay channel is not changed. The energy scale μ is actually the Higgs-boson energy, representing the total energy of final states, e.g., two-photon state and four-lepton states, into which the produced Higgs boson decays.

These discussions imply that the resonant amplitude (number of events) of two-photon invariant mass $m_{\gamma\gamma} \approx 126\,\text{GeV}$ and/or four-lepton invariant mass $m_{4l} \approx 126\,\text{GeV}$ is expected to become smaller as the produced Higgs-boson energy μ increases, i.e., the energy of final two-photon and/or four-lepton states increases, when the CM energy $\sqrt{s}$ of LHC pp collisions increases with a given luminosity. Suppose that the total decay rate or each channel decay rate of the SM Higgs boson is measured at the Higgs-boson energy $\mu = m_t$ and the SM value of Yukawa coupling $\bar{g}_t^2(m_t) = 2m_t^2/v \approx 1.04$, see figure 2. In the scenario of tightly-bound composite Higgs boson, as the Higgs-boson energy μ increases to $\mu = 2m_t$, the Yukawa coupling $\bar{g}_t^2(2m_t) \approx 0.98$, the variation of total decay rate or each channel decay rate is expected to be 6% for $\Delta \bar{g}_t^2 \approx 0.06$. Analogously, the variation is expected to be 9% at $\mu = 3m_t$, $\bar{g}_t^2(3m_t) \approx 0.95$ or 11% at $\mu = 4m_t$, $\bar{g}_t^2(4m_t) \approx 0.93$, as shown in figure 2. These variations are still too small to be clearly distinguished by the present LHC experiments. Such scenario of tightly-bound composite Higgs boson has not been found so far any tension with electroweak precision variables. Nevertheless, it certainly needs more detailed analysis of the tightly-bound composite Higgs phenomenology in comparison with electroweak precision variables in future work.

In addition, the nonresonant new phenomena, stemming from four-fermion scattering amplitudes of diemnsion-6 irrelevant operators in effective Lagrangian (2.6), are hightly suppressed $\mathcal{O}(\Lambda^{-2})$ and thus hard to be identified [21] in high-energy processes of LHC pp collisions (e.g., the Drell-Yan dilepton process, see ref. [52]), e^-e^+ annihilation to hadrons and deep inelastic lepton-hadron e^-p scatterings at TeV scales. Nonetheless, these effects are the nonresonant new signatures of low-energy collider that show the deviations of such scenario from the SM.

3.1.3 Yukawa couplings and FCNC's in IR-domain

The SSB generated top-quark mass $m_t \propto \bar{g}_t v$ breaks chiral symmetries, fermion-family mixing matrices (2.14) become relevant for coupling different fermion families. As a consequence, other quarks and leptons acquire their masses $\bar{g}_f v$, because Schwinger-Dyson (SD) equations for their self mass-energy functions acquire the explicit symmetry breaking (ESB) terms induced by the $W^\pm$-boson vector-like couplings and quark-lepton interactions at high energies, via the fermion-family mixing matrices like the CKM (2.14) and PMNS

matrices in the SM. References [12, 13] show in details how the top quark acquires its mass together with Higgs boson mass by the SSB in terms of $\bar{g}_t(\mu)$ and $\tilde{\lambda}(\mu)$ couplings (figures 2), and other SM fermions acquire their masses $m_f \propto \bar{g}_f v$ by the ESB, as functions of the top-quark mass m_t or Yukawa coupling $\bar{g}_t(\mu)$, and mixing-matrix elements of the CKM and PMNS types in the SM, which are intrinsic parameters fixed by experiments. The hierarchy patterns of fermion masses and mixing-matrix elements are closely related.

As a consequence, the SM chiral gauge symmetries and global fermion-family (flavor) symmetries are broken at a soft energy scale $m^f = \bar{g}_t v \ll \mathcal{E} \ll \Lambda$. The latter fermion-family $U_L(3) \times U_R(3)$ symmetries are broken to the U(1) symmetry for each fermion family, i.e., $U_1(1) \times U_2(1) \times U_3(1)$. Thus the quadrilinear four-fermion operators (2.10), bilinear two-fermion operators (2.11) and (2.12) are "diagonal", namely they are for each fermion family without any fermion-family mixing in the fermion-family space based on mass eigenstates of fermions. Given a definite electric charge, the U(1)-symmetry for each fermion flavor is still preserved and the quantum number of each fermion flavor is conserved. This completely prohibits any *four-fermion-interacting* process that violates fermion-flavor-number conservation, such as the FCNC process converting from one elementary fermion flavor ψ^f to another $\psi^{f'}$ with the same electric charge.

However, such prohibition is relaxed as perturbatively turning on the interactions (2.6) between chiral-gauge-boson $W^\pm$ and massive fermions in addition to the four-fermion interactions (2.10). The reason is that these chiral-gauge interactions are not diagonal in the fermion-family space based on the mass eigenstates of fermions (2.11) and (2.12), attributed to the fact that the mass eigenstates of the SM *elementary* fermions are different from their chiral-gauge eigenstates. As a result, a 1PI-interacting vertex that violates the fermion-flavor-symmetry $U_1(1) \times U_2(1) \times U_3(1)$ is induced via the mixing matrices of CKM type (2.14) and interactions among SM gauge bosons, e.g. $W^\pm$ and photon, at one-loop level. Such 1PI vertex allows the FCNC processes of changing one *elementary* fermion ψ^f flavor [mass eigenstate (2.8) or (2.9)] to another *elementary* fermion $\psi^{f'}$ flavor [mass eigenstate] with the same electric charge. This situation is the same as that of the SM with an elementary Higgs boson.

Nevertheless, such $W^\pm$-boson contributions of SM-type to the FCNC processes are highly suppressed, since they come from the loop-level contributions of the SM $W^\pm$-boson via the fermion-family mixing matrix of the CKM type (2.14) in its gauge coupling vertexes. In conclusion, apart from the SM-type suppressed contributions to FCNC, the effective Lagrangian (2.6) with four-fermion operators (2.10) in the IR-domain does not contain any additional unsuppressed 1PI vertexes that contribute to the FCNC processes.

3.2 Gauge-symmetric phase of strong four-fermion coupling

We turn to the brief recall on the gauge-symmetric phase of strong four-fermion coupling G,

$$- G \bar{\psi}_L \psi_R \bar{\psi}_R \psi_L, \tag{3.8}$$

preserving $SU_L(2)$ gauge symmetry, where two-component Weyl fermion ψ_L (ψ_R) is an $SU_L(2)$ doublet (singlet). The strong-coupling expansion was adopted to calculate two-point functions of composite boson and fermion fields [14, 15], and the vertex functions of

their couplings to the $SU_L(2)$-gauge bosons [16–19]. Detailed calculations can be found in these references and their appendices. In the lowest non-trivial order, we obtained the propagators of the massive composite bosons $\mathcal{A} = (\bar{\psi}_R \psi_L)$ and composite Dirac fermions: $\Psi_D = (\psi_L, \mathcal{A}\psi_R)$ and $\Psi_S = (\mathcal{A}^\dagger \psi_L, \psi_R)$,

$$\langle \mathcal{A}(0)\mathcal{A}^\dagger(x) \rangle \Rightarrow \frac{Z_B^S}{q^2 + M_B^2}; \quad \langle \Psi_{D,S}(0)\bar{\Psi}_{D,S}(x) \rangle \Rightarrow Z_{D,S}^S \frac{ip^\mu \gamma_\mu + M_{D,S}}{p^2 + M_{D,S}^2}, \qquad (3.9)$$

where the pole $M_{B,D,S}$ and residue $Z_{B,D,S}^S$ respectively represent mass and form factor of composite particles. As long as their form-factors are finite, these composite particles behave as elementary particles. The propagators of renormalized composite particles (3.9) give their mass-shell conditions,

$$E_B = \sqrt{q^2 + M_B^2} \approx M_B, \quad E_{D,S} = \sqrt{p^2 + M_{D,S}^2} \approx M_{D,S}, \quad \text{for} \;\; q^2, p^2 \ll M_{B,D,S}^2. \;\; (3.10)$$

The vertex functions of their $SU_L(2)$-couplings were obtained by Ward identities from propagators (3.9), because the composite-particle spectra preserve the $SU_L(2)$-gauge symmetry.

These massive composite particles formed by the such strong-coupling dynamics in the gauge-symmetric phase are completely different from the composite particles like massive Higgs boson and massless Goldstone bosons formed by the weak-coupling NJL dynamics in the symmetry-breaking phase where the SSB takes place.

3.3 Strong critical coupling and the UV-stable fixed point

This indicates that there are two distinct phases: (i) the symmetry-breaking phase $G_c < G < G_{\text{crit}}$ for the SM of elementray particles; (ii) the gauge-symmetric phase $G > G_{\text{crit}}$ for an effective theory of composite particles, and the second-order phase transition from one phase to another at the strong critical coupling G_{crit}.

3.3.1 Strong critical coupling

In the symmetric phase, we indeed found [14, 15] the existence of strong critical coupling G_{crit} by using strong four-fermion coupling expansion to approximately calculate the two-point Green function (3.9) of composite boson and examine sign change of quadratic term $M_B^2 \mathcal{A}\mathcal{A}^\dagger(x)$. Instead, based on the symmetry-breaking phase of weak four-fermion coupling, see section 3.1, we show the existence of strong critical point G_{crit} of the second-order phase transition from the symmetry-breaking phase to gauge-symmetric phases.

In refs. [20, 51], we solve the full one-loop RG equations [28] for running couplings $\bar{g}_t(\mu^2)$ and $\bar{\lambda}(\mu^2)$ with the top-quark and Higgs-boson mass-shell conditions

$$m_t = \bar{g}_t(m_t)v/\sqrt{2}, \quad m_H^2/2 = \tilde{\lambda}(m_H)v^2, \qquad (3.11)$$

$m_t \approx 172.9\,\text{GeV}$ and $m_H \approx 126\,\text{GeV}$ fixed by experiments. As a result, we uniquely determine the renormalized form factor $\tilde{Z}_H(\mu)$ and quartic coupling $\tilde{\lambda}(\mu)$ of the composite

Higgs particle. We also find the intermediate energy scale $\mathcal{E}$, at which the effective quartic coupling $\tilde{\lambda}(\mathcal{E}) = 0$, and the finite value of form-factor $\tilde{Z}_H(\mathcal{E})$,

$$\mathcal{E} \approx 5.1 \text{ TeV}, \quad \tilde{Z}_H(\mathcal{E}) \approx 1.26, \quad \tilde{\lambda}(\mathcal{E}) = 0, \tag{3.12}$$

otherwise the effective theory would run into an instability ($\tilde{\lambda} \sim 0^-$) beyond $\mathcal{E}$. These are certainly preliminary and qualitative results, since we use one-loop RG equations in low-energy and weak-coupling region and extrapolate their solutions to high-energy and strong-coupling region. Nevertheless, the solution (3.12) implies the following three important features. (i) In the effective Lagrangian of quadratic term $m_H^2 HH^\dagger/2$, the squared Higgs-boson mass $m_H^2 = 2\tilde{\lambda}(\mu)v^2$ changes its sign at $\mu = \mathcal{E}$, indicating the second-order phase transition G_{crit} from the symmetry-breaking phase to a gauge-symmetric phase of high-energy and strong-coupling region. (ii) The form-factor $\tilde{Z}_H(\mu) \neq 0$ shows that the tightly bound composite Higgs particle behaves as if an elementary particle for $\mu \leq \mathcal{E}$. (iii) The effective form-factor $\tilde{Z}_H(\mathcal{E})$ of composite Higgs boson is finite, implying the formation of massive composite fermions $\Psi \sim (H\psi)$ in the gauge-symmetric phase.

To close this subsection, it is worthwhile to mention that in ref. [53] it is shown in the elementary Higgs-boson model that the quadratic term from high-order quantum corrections has a physical impact on the SSB and the phase transition to a symmetric phase occurs at the scale of order of TeV.

3.3.2 UV-stable fixed point

In order to show that this critical point G_{crit} of the second-order phase transition can be a UV-fixed point, we calculated the β-function in the symmetric phase of strong four-fermion coupling. Up to the lowest non-trivial order of the strong coupling expansion, i.e., the two-fermion-loop contribution (sun-set diagrams), and we obtained the negative β-function [20]

$$\beta(G) = p^2 \frac{\partial \mathcal{G}(p)}{\partial p^2} \approx \frac{6}{\mathcal{G}} \frac{\partial \Phi(p^2/\Lambda^2)}{\partial \ln(p^2/\Lambda^2)} < 0, \tag{3.13}$$

where $\mathcal{G} \equiv G \times (\Lambda/\pi)^2$ and the dimensionless Lorentz-scalar function $\Phi(p^2/\Lambda^2)$ is positive and finite, monotonically decreases as the energy scale p^2/Λ^2 increases. On the basis of the $\beta(G)$-function being positive (3.4) and becoming negative (3.13), as sketched as "I", "II" and "III" in figure 1, we infer there must be at least one zero-point of the $\beta(G)$-function, i.e., $\beta(G_{\text{zero}}) = 0$ and $\beta'(G_{\text{zero}}) < 0$. This zero-point G_{zero} is a UV-stable fixed point, which should coincide with the strong critical coupling $G_{\text{zero}} \approx G_{\text{crit}}$ for the reason that a UV-stable fixed point should be the candidate of the critical point G_{crit} for the second-order phase transition from the symmetry-breaking phase to the symmetric phase. As the running energy scale μ increases, the effective coupling $G(\mu) \to G_{\text{crit}} \pm 0$ (thin right and left arrows, see figure 1) is attracted to this UV-stable fixed point from both symmetry-breaking and symmetric phases. In the scaling region (vicinity) of UV-stable fixed point G_{crit}, i.e., UV-domain, RG flow approaches to the UV-fixed point, as energy scale μ increases, in the scenes of renormalization group (scaling) invariance and resultant RG equations.

This is analogous to non-linear σ models [54], which contain a dimensionful coupling constant and are thus not perturbatively renormalizable. Nevertheless, the nonperturbative critical coupling of these σ models shows the second-order phase transition from the ordered (symmetry-breaking) phase to the disordered (symmetric) phase, and exhibits a non-trivial UV-fixed point and UV-scaling domain of the renormalization group both in the lattice formulation [55, 56] and in the $2 + \epsilon$ formulation [57, 58].

However, due to the lack of a non-perturbative method to effectively approach to the critical coupling G_{crit} and its neighborhood, we have not been able to quantitatively determine the G_{crit} value and properties of its scaling region i.e., the UV-domain, which will be qualitatively discussed and recalled in next section.

3.4 The UV-domain of UV-stable fixed point

3.4.1 Energy threshold of composite particles

As the running energy scale μ decreases in the vicinity of UV-stable fixed point G_{crit}, the $\beta(\mu)$ function (see figure 1) shows that the RG flows take the effective theory of composite particles away from the UV fixed point towards the IR-domain of the IR-fixed point G_c, where the low-energy SM of elementary particle physics is realized. This implies the existence of the energy threshold $\mathcal{E}_{\mathrm{thre}}$, below which $\mu < \mathcal{E}_{\mathrm{thre}}$ composite particle dissolves into its constituents of SM elementary particles. As discussed in sections V and VI of refs. [17, 18], when the energy scale μ decreases to the energy threshold $\mathcal{E}_{\mathrm{thre}}$ and $G(\mu) \to G_{\mathrm{crit}}(\mathcal{E}_{\mathrm{thre}})$, the phase transition occurs from the symmetric phase to the symmetry-breaking phase, all composite particles (poles) dissolve into their constituents, which are represented by three-fermion, fermion-boson and two-fermion cuts in the energy-momentum plane, as their form factor and binding energy vanish [59–62]. Actually, the energy threshold $\mathcal{E}_{\mathrm{thre}}$ represents the symmetry-breaking scale at the second-order phase transition G_{crit}.

The composite-particle masses M (3.10) contain the negative binding energy $-\mathcal{B}[G(\mu)]$ and positive kinetic energies $\mathcal{K}$ of their constituents. The energy threshold $\mathcal{E}_{\mathrm{thre}}$ is determined by $\mathcal{B}[G(\mu)]_{\mu \to \mathcal{E}_{\mathrm{thre}}} \to \mathcal{K}$ and vanishing form factors of composite particles in the symmetric phase. These calculations require non-perturbative approaches that need to be developed in future. Nevertheless, we gain some physical insight into the symmetry-breaking scale $\mathcal{E}_{\mathrm{thre}} \gtrsim \mathcal{E} \approx 5.1 \,\mathrm{GeV}$, since the approximate $\mathcal{E}$-value (3.12) is obtained in symmetry-breaking phase by extrapolating the solutions of the one-loop RG-equations of low-energy (v) region to high-energy ($\mathcal{E}$) region.

3.4.2 Characterisic energy scale

In the IR-domain of the fixed point G_c where the effective Lagrangian of the SM is realized, the correlation length ξ_v corresponding to the electroweak scale $v = 239.5 \,\mathrm{GeV}$ that is attributed to the SSB dynamics in symmetry-breaking phase sets the physical energy scale of IR-domain. This characteristic energy scale is much smaller than the cutoff ($v \ll \Lambda$), leading to the renormalization group (scaling) invariance and resultant RG equations in the IR-domain. This characteristic electroweak scale v is determined by the experimental measurements of intermediate gauge bosons $W^{\pm}$ and Z^0 masses.

Analogously, as discussed in ref. [20], in the UV-domain (scaling region) of the UV-fixed point (critical point) $G_{\rm crit}$ of the second-order phase transition, the correlation length ξ or characteristic energy $\mathcal{E}_\xi = \xi^{-1}$ sets the physical scale. The correlation length ξ is much larger than the cutoff $a \approx \Lambda^{-1}$, i.e., $\xi \gg a$ or $\mathcal{E}_\xi \ll \Lambda$ leads to the renormalization group (scaling) invariance and resultant RG equations in the UV-domain. In this scaling domain, the running coupling $G(a/\xi)$ can be expanded as a series,

$$G(a/\xi) = G_{\rm crit}\left[1 + a_0(a/\xi)^{1/\nu} + \mathcal{O}[(a/\xi)^{2/\nu}]\right] \to G_{\rm crit} + 0^+, \tag{3.14}$$

for $a/\xi \ll 1$, leading to the β-function

$$\beta(G) = (-1/\nu)(G - G_{\rm crit}) + \mathcal{O}[(G - G_{\rm crit})^2] < 0. \tag{3.15}$$

The correlation length ξ follows the scaling law

$$\xi = c_0 a \exp \int^G \frac{dG'}{\beta(G')} = \frac{c_0 a}{(G - G_{\rm crit})^\nu}, \tag{3.16}$$

where the coefficient $c_0 = (a_0 G_{\rm crit})^\nu$ and critical exponent ν need to be determined by non-perturbative numerical simulations. The physical scale $\mathcal{E}_\xi \equiv \xi^{-1}$ in the UV-domain is attributed to the strong-coupling dynamics of forming composite particles. This implies the masses of composite particles (3.9) and (3.10)

$$M \propto \mathcal{E}_\xi = \xi^{-1}, \tag{3.17}$$

and the running coupling $G(\mu)|_{\mu \to \mathcal{E}_{\rm thre}+0^+} \to G_{\rm crit}$,

$$G(\mu) \simeq G_{\rm crit}\left[1 - \frac{1}{\nu}\ln\left(\frac{\mu}{\mathcal{E}_\xi}\right)\right]^{-1}, \quad \mu/\mathcal{E}_\xi = \xi/(aa_0^\nu) > 1, \tag{3.18}$$

and the scale μ indicates the energy transfer between constituents inside composite particles.

On the basis of these discussions and observations, we advocate the following relation for (i) the energy scale $\mathcal{E} \approx 5$ TeV of eq. (3.12) extrapolated by the RG equations in the IR-domain for the SM, (ii) the energy threshold $\mathcal{E}_{\rm thre}$ corresponding to the phase-transition scale from symmetric to symmetry-breaking phases and (iii) the characteristic energy scale $\mathcal{E}_\xi$ in the UV-domain for the effective theory of composite particles

$$\mathcal{E} \lesssim \mathcal{E}_{\rm thre} \lesssim \mathcal{E}_\xi \ll \Lambda, \quad \mathcal{E} \approx 5\,{\rm TeV}. \tag{3.19}$$

The values of these characteristic scales of UV-domain need some experimental knowledge in high energies, analogously to the electroweak scale (v) of IR-domain.

3.5 Relevant and irrelevant operators in IR- and UV-domains

In the weak-coupling IR-domain, as an energetically favorable solution for the SSB ground state [50], among four-fermion operators (2.6) the top-quark channel $G(\bar{\psi}_L^{ia} t_{Ra})(\bar{t}_R^b \psi_{Lib})$ [28] is the only physically relevant and renormalizable operators of effective dimension-4, due

to the NJL-dynamics for the SSB. Namely, it becomes the effective SM Lagrangian (3.1) with *bilinear* top-quark mass term and Yukawa coupling to the composite Higgs boson H, which obeys the RG equation approaching to the low-energy SM physics characterized by the energy scale $v \approx 239.5 \, \text{GeV}$. Other four-fermion operators in eq. (2.6), as well as repulsive four-fermion operators (2.4), do not undergo the SSB and are irrelevant dimension-6 operators, whose tree-level amplitudes of four-fermion scatterings are suppressed $\mathcal{O}(\Lambda^{-2})$, thus their deviations from the SM could not be experimentally accessible today.

In the strong-coupling UV-domain, all attractive four-fermion operators (2.6) are physically relevant operators associating to the strong-coupling dynamics and formation of composite bosons and fermions (3.9). Due to the unique four-fermion coupling G, this strong-coupling dynamics of forming composite particles occurs in all channels of eq. (2.6) for each SM fermion family. These composite particles on mass-shells behave as if they were elementary, as long as their form factors are finite. All 1PI functions $\Gamma[\mu, G(\mu)]$ of the quantum field theory (2.6) at the UV-cutoff scale Λ evolve to either irrelevant or relevant 1PI functions, as the running energy scale μ increases. The irrelevant 1PI functions are suppressed by powers of $(\mathcal{E}_\xi/\Lambda)^n$ and thus decouple from the effective theory. Instead, the relevant 1PI functions follow the scaling law (RG equations), therefore are effectively dimension-4 and renormalizable, for example the propagators of composite fermions and bosons and their vector-like coupling vertexes to the SM gauge bosons. The effective field theory in this UV-domain is expected to contains the massive composite particle spectrum preserving the SM chiral gauge symmetries, and relevant operators of effective dimension-4 following the RG equations. Compared with the SM in the IR-domain, the effective theory of composite particles in the UV-domain has the same chiral gauge symmetries (quantum numbers) and couplings to gauge bosons ($\gamma, W^\pm, Z^0$ and gluon), but the different vector-like spectra and coupling vertexes, apart from massive composite particles being comprised by SM elementary particles. Some of these peculiar features and their possible experimental implications were studied in refs. [12, 20, 21]. These are the properties of effective composite-particle theory in the UV-domain that we attempt to study in this article and in future.

To end this section, it is worthwhile to note that the repulsive four-fermion operators (2.4) are irrelevant operators of dimension-6, and thus suppressed $\mathcal{O}(\Lambda^{-2})$ for the reasons that they are neither associated with the NJL dynamics of the SSB in the IR-domain, nor associated with the strong-coupling dynamics of forming composite particles in the UV-domain.

It is also worthwhile to mention that these discussions are reminiscent of the asymptotic safety [63, 64] that quantum field theories regularized at UV-cutoff Λ might have a non-trivial UV-stable fixed point, RG flows are attracted into the UV-stable fixed point with a finite number of physically renormalizable operators. The weak and strong four-fermion coupling G brings us into two distinct domains. This lets us also recall the quantum chromodynamics (QCD): asymptotically free quark states in the domain of a UV-stable fixed point and bound hadron states in the domain of a possible IR-stable fixed point.[4]

---

[4]The references on this issue can be found in the recent paper: Z.-Y. Zheng and G.-L. Zhou, "A method for getting well-defined coupling constant in all region", arXiv:1705.07430.

4 Composite particles and effective Lagrangian in UV-domain

In the gauge symmetric phase of an $SU_L(2)$-chiral gauge theory containing the four-fermion operator (3.8), the composite particles and 1PI vertex functions, as well as their properties in the UV-domain were analyzed by using the approach of strong-coupling expansion to the dynamics of four-fermion operators at the cutoff Λ [14, 15, 17–21]. In this section, however, based on the effective Einstein-Cartan Lagrangian (2.6) in the SM framework, see section 2.4, we are going to show the composite-particle spectrum and 1PI interaction (effective Lagrangian) in terms of the quantum numbers of SM gauge symmetries. The purpose is that we shall go further to discuss composite particles decay and other processes into SM elementary gauge bosons and fermions, relevantly to possible high-energy experiments. These are the main results of this article presented in this section and following sections 5, 6 and 7.

4.1 Composite particles in UV-domain

4.1.1 Quark sector

Performing strong-coupling calculations similar to those detailedly presented in the refs. [14, 15] and their appendices, we obtain the following results. For the u-quark channel, the massive composite boson is an $SU_L(2)$-doublet

$$\mathcal{A}^i = [Z_\Pi^S]^{-1/2}(\bar{u}_{Ra}\psi_L^{ia}) \tag{4.1}$$

of the hypercharge $Y = -1/2$ and $i(a)$ being the weak isospin (color) index. This composite boson combines with an elementary two-component Weyl quark to form the composite two-component Weyl-fermion states (three-fermion states),

$$\mathbf{\Psi}_R^{ib} = (Z_R^S)^{-1}\mathcal{A}^i u_R^b; \quad \mathbf{\Psi}_L^b = (Z_L^S)^{-1}\mathcal{A}^{i\dagger}\psi_{iL}^b, \tag{4.2}$$

and to form the massive composite four-component Dirac-fermion states: the $SU_L(2)$ doublet $\mathbf{\Psi}_D^{ib}$ and the $SU_L(2)$ singlet $\mathbf{\Psi}_S^b$,[5]

$$\mathbf{\Psi}_D^{ib} = (\psi_L^{ib}, \mathbf{\Psi}_R^{ib}), \qquad \mathbf{\Psi}_S^b = (\mathbf{\Psi}_L^b, u_R^b). \tag{4.3}$$

The form factors $[Z_\Pi^S]^{1/2}$ (4.1) and $Z_{R,L}^S$ (4.2) are generalized wave-function renormalizations of the composite boson and fermion operators.

The four-component composite Dirac fermions are vector-like spectra, fully preserving the parity symmetry. The composite $SU_L(2)$ doublets $\mathbf{\Psi}_D^{ib}$ carry the same $U_Y(1)$-hypercharge as the SM elementary and left-handed $SU_L(2)$ doublets ψ_L^{ib}. The composite $SU_L(2)$ singlets $\mathbf{\Psi}_S^b$ carry the same $U_Y(1)$-hypercharge as the SM elementary and right-handed $SU_L(2)$ singlets u_R^b. These composite particles have the SM-gauge symmetric masses

$$M_\Pi^2\mathcal{A}^{i\dagger}\mathcal{A}^i, \quad M_F\bar{\mathbf{\Psi}}_D^{ib}\mathbf{\Psi}_D^{ib}, \quad \text{and} \quad M_F\bar{\mathbf{\Psi}}_S^b\mathbf{\Psi}_S^b. \tag{4.4}$$

---

[5]A four-component composite Dirac fermion composes an elementary Weyl fermion and a composite Weyl fermion, each of them is two-component, either left- or right-handed (a definite chirality) [14, 15], similar discussions for massive composite bosons, see ref. [20].

For the d-quark channel, the composite particles are represented by eqs. (4.1)–(4.3) with the replacement $u_{Ra} \to d_{Ra}$. In this case, $\mathcal{A}^i$ has the $U_Y(1)$-hypercharge $Y = 1/2$. $\boldsymbol{\Psi}_L^b$ and $\boldsymbol{\Psi}_S^b$ have the same $U_Y(1)$-hypercharge as the quark field d_R^b. $\boldsymbol{\Psi}_R^{ib}$ and $\boldsymbol{\Psi}_D^{ib}$ have the same $U_Y(1)$-hypercharge, i.e., the $U_Y(1)$-hypercharge of the SM quark fields ψ_L^{ib}.

This represents the first family of the composite particles composed by the SM elementary particles (quarks) in the first family. The composite boson and fermion states (4.1)–(4.3) are the eigenstates of both the SM gauge interactions and mass operators (4.4), due to the SM gauge symmetries are preserved by the massive spectra of composite particles. The same discussions also apply for the second and third quark families by substituting the $SU_L(2)$ doublet (u_{La}, d_{La}) into (c_{La}, s_{La}) or (t_{La}, b_{La}) and singlet u_{Ra} into t_{Ra} or c_{Ra}, as well as singlet d_{Ra} into b_{Ra} or s_{Ra}.

4.1.2 Lepton sector

In the lepton sector, the composite boson and Weyl-fermion states formed by the first term (ℓ_R-channel) of eq. (2.16) are:

$$\mathcal{A}^i = [Z_H^S]^{-1/2}(\bar{\ell}_R \ell_L^i); \qquad \boldsymbol{\Psi}_R^i = [Z_R^S]^{-1}\mathcal{A}^i \ell_R, \quad \boldsymbol{\Psi}_L = [Z_L^S]^{-1}\mathcal{A}^{i\dagger}\ell_{iL}, \qquad (4.5)$$

and the massive composite Dirac fermions $\boldsymbol{\Psi}_D^i = (\ell_L^i, \boldsymbol{\Psi}_R^i)$ and $\boldsymbol{\Psi}_S = (\boldsymbol{\Psi}_L, \ell_R)$. The composite boson doublets $\mathcal{A}^i = [Z_H^S]^{1/2}(\bar{\ell}_R \ell_L^i)$ carry the hypercharge $Y = 1/2$, the doublets $\boldsymbol{\Psi}_D^i = (\ell_L^i, \boldsymbol{\Psi}_R^i)$ carry the $U_Y(1)$ hypercharge of the SM field ℓ_L^i and the singlets $\boldsymbol{\Psi}_S = (\boldsymbol{\Psi}_L, \ell_R)$ carry the $U_Y(1)$ hypercharge of the SM field ℓ_R. Compared with their counterparts (4.1)–(4.3) in the quark sector, these massive composite particles have different quantum numbers of the SM gauge symmetries. The composite particles formed by the second term (ν_R^ℓ-channel) of eq. (2.16) are obtained by eq. (4.5) with the replacement $\ell_R \to \nu_R^\ell$. In this case, $\mathcal{A}^i$ has the $U_Y(1)$-hypercharge $Y = -1/2$. $\boldsymbol{\Psi}_L$ and $\boldsymbol{\Psi}_S$ have the $U_Y(1)$ hypercharge of the right-handed neutrino ν_R. $\boldsymbol{\Psi}_L^i$ and $\boldsymbol{\Psi}_D^i$ have the same $U_Y(1)$ hypercharge, i.e., the $U_Y(1)$ hypercharge of the SM lepton field ℓ_L^i.

4.1.3 Quark-lepton sector

Analogously, we present for the d_R^a- and e_R-channel of quark-lepton interactions (2.18), the massive composite Dirac fermions: $SU_L(2)$ doublet $\boldsymbol{\Psi}_D^i = (\ell_L^i, \boldsymbol{\Psi}_R^i)$ and singlet $\boldsymbol{\Psi}_S = (\boldsymbol{\Psi}_L, e_R)$, where the renormalized composite boson and composite Weyl-fermion states are:

$$\mathcal{A}^i = [Z_H^S]^{-1/2}(\bar{d}_R^a \psi_{La}^i); \quad \boldsymbol{\Psi}_R^i = [Z_R^S]^{-1}\mathcal{A}^i e_R, \quad \boldsymbol{\Psi}_L = [Z_L^S]^{-1}\mathcal{A}^{i\dagger}\ell_{iL}, \qquad (4.6)$$

which respectively carry the $U_Y(1)$-hypercharge: $Y = 1/2$, $Y = -1/2$ and $Y = -1$. For the ν_R^e-channel, the composite particles are represented by eq. (4.6) with the replacements $e_R \to \nu_R^e$ and $d_R^a \to u_R^a$. In this case, the counterparts of the composite states (4.6) respectively carry the $U_Y(1)$-hypercharge: $Y = -1/2$, $Y = -1/2$ and $Y = 0$.

The composite particles from the second and third lepton families can be obtained by substitutions: $e \to \mu, \tau$, $\nu^e \to \nu^\mu, \nu^\tau$, and $u \to c, t$ and $d \to s, b$. In general, the $U_Y(1)$-hypercharge Y and $U_{\rm em}$-electric charge Q_i of the composite particle is the sum of its constituents' hypercharges and electric charges, obeying the relation $Q_i = Y + t_{3L}^i$ in units of e, where t_{3L}^i is the diagonal third component of $SU_L(2)$-isospin, $t_{3L}^1 = 1/2$ for the neutrino and up quarks, and $t_{3L}^2 = -1/2$ for the electron and down quarks.

4.1.4 Discussions and three-family replication

In the quark and lepton sectors, the massive composite boson $\mathcal{A}^i$, the massive composite Dirac fermions $SU_L(2)$ doublet Ψ_D^i and singlet Ψ_S carry an electric charge $Q = (2/3, -1/3, -1, 0)$ for u_R^a- and d_R^a-quark channels, e_R- and ν_R-lepton channels respectively. In the quark-lepton sector, the massive composite boson $\mathcal{A}^i$, the massive composite Dirac fermions $SU_L(2)$ doublet Ψ_D^i and singlet Ψ_S carry an electric charge $Q = (2/3, -1/3, -1, 0)$ for the d_R^a-e_R channel and u_R^a-ν_R channel respectively. It should be mentioned that the composite bosons $\mathcal{A}^i$ carry neither the baryon number nor the lepton number, whereas the composite fermions Ψ_D^i and Ψ_S carry the baryon or the lepton number of the SM elementary fermions.

These first-family composite particles are composed only by the SM elementary particles in the first family, and there are no extra elementary gauge bosons and fermions, except the right-handed sterile neutrino ν_R. The second-family (third-family) composite particles are composed only by the SM elementary particles in the second (third) family. The three families of composite particles are replicated corresponding to the three families of elementary fermions in the SM.

Though composite particles are massive, they carry the quantum numbers of the SM chiral gauge symmetries, which are the sum of quantum numbers of their constituents of the SM elementary particles. The propagators of these composite particles have poles and residues that respectively represent their masses and form factors [14–18]. As long as their form factors are finite, these composite particles behave as elementary particles. It should be mentioned that the gauge symmetric masses $M_{\Pi,F}$ and form factors $Z_{\Pi,L,R}^S$ of composite particles, e.g., (4.1)–(4.4) can be different from one to another, due to some other effects that we do not study here.

To end this section, we present some discussions on the third-family composite bosons (4.1) by the top and bottom quarks, compared with the composite Higgs and Goldstone bosons. The former comprises of the massive bound states $(\bar{t}t)^s$, $(\bar{t}\gamma_5 t)^s$ and $(\bar{t}\gamma_5 b)^s$ formed by the strong-coupling dynamics in the UV-domain of the symmetric phase. They are different from the composite massive Higgs boson $H = (\bar{t}t)$ and massless Goldstone bosons $(\bar{t}\gamma_5 t)$ and $(\bar{t}\gamma_5 b)$ [28] formed by the NJL dynamics in the IR-domain of the symmetry-breaking phase. Nevertheless, at the strong critical point G_{crit} of second-order phase transition that may occur around the scale $\mathcal{E}_\xi$, see eq. (3.12), from the point view of the different ground states of the symmetric phase and the symmetry-breaking phase, we expect some relationships of the binding energies and form factors between two types of composite bosons, e.g., $(\bar{t}t)^s$ and $(\bar{t}t)$, with the same SM quantum numbers. We will study this issue and its experimental implications in future.

4.2 Effective Lagrangian of composite particles in UV-domain

4.2.1 SM effective Lagrangian of elementary particles in IR-domain

To compare and contrast with the effective Lagrangian of composite particles in the UV-domain of the symmetric phase, we also present the effective SM Lagrangian in the IR-domain of the symmetry-breaking phase. The well-studied SM effective Lagrangian of

elementary fermions in the first family reads

$$\mathcal{L}_{\rm SM} = \sum_i \bar{\psi}^i (i\gamma_\mu \partial_\mu - m_i - m_i H/v)\psi^i - e\sum_i Q_i \bar{\psi}^i \gamma^\mu \psi^i A_\mu$$
$$- \frac{g_2}{2\sqrt{2}} \sum_i \bar{\psi}^i \gamma^\mu (1 - \gamma_5)(T^+ W_\mu^+ + T^- W_\mu^-)\psi^i$$
$$- \frac{g_2}{2\cos\theta_W} \sum_i \bar{\psi}^i \gamma^\mu (g_V^i - g_A^i \gamma_5)\psi^i Z_\mu \; + \; {\rm Higgs\;\; sector}, \qquad (4.7)$$

for the both quark and lepton sector in one SM family, where i is the $SU_L(2)$-isospin index, $T^\pm$ is the weak isospin raising and lowering operators $g_V^i = t_{3L}^i - Q_i \sin^2\theta_W$ and $g_A^i = t_{3L}^i$. The weak angle $\theta_W = \tan^{-1}(g_1/g_2)$ and the electron electric charge $e = g_2 \sin\theta_W$. These massive fermions couple to the massless photon A_μ, massive intermediate gauge bosons $W_\mu^\pm$ and Z_μ. The gauge and mass eigenstates of the SM elementary fermions are different, leading to the fermion-family mixing, when three fermion families are considered. The phenomenological Yukawa couplings $\bar{g}_i = m_i/v$ of Higgs boson and elementray fermion ψ_i of mass m_i are related to the top-quark Yukawa coupling $\bar{g}_t$ of eq. (3.1) discussed in section 3.1, and see refs. [12, 13] for some details.

4.2.2 Effective Lagrangian of composite particles in UV-domain

In the UV-domain of the symmetric phase, massive composite bosons and fermions (see section 4.1) have the quantum numbers of SM chiral gauge symmetries $SU_c(3) \times SU_L(2) \times U_Y(1)$, couplings g_1, g_2, g_3 to SM gauge bosons $\gamma, W^\pm, Z^0$ and gluon. The spectrum of these massive composite bosons and fermions preserves the SM chiral gauge symmetries. The gauge and mass eigenstates of massive composite bosons and fermions are the same. The interacting 1PI vertexes of composite particles and SM gauge bosons can be obtained by Ward identities associating to SM gauge symmetries.[6] As a result, at tree-level we obtain the following effective Lagrangian for the first-family composite particles (4.1), (4.3), (4.5), (4.6).

For the massive composite Dirac fermions Ψ_D^i and Ψ_S (4.1)–(4.4) the u_R-quark channel in the quark sector, the effective Lagrangian reads

$$\mathcal{L} = \sum_i \bar{\Psi}_D^i (i\gamma^\mu \partial_\mu - M_D^i)\Psi_D^i + \bar{\Psi}_S (i\gamma^\mu \partial_\mu - M_S)\Psi_S$$
$$- e\sum_i Q_i (\bar{\Psi}_D^i \gamma^\mu \Psi_D^i) A_\mu - (2/3)e(\bar{\Psi}_S \gamma^\mu \Psi_S) A_\mu$$
$$- \frac{g_2}{\sqrt{2}} \sum_i \bar{\Psi}_D^i \gamma^\mu (T^+ W_\mu^+ + T^- W_\mu^-)\Psi_D^i$$
$$- \frac{g_2}{2\cos\theta_W} \left\{ \sum_i \bar{\Psi}_D^i \gamma^\mu (g_V^i + g_A^i)\Psi_D^i + \bar{\Psi}_S \gamma^\mu (g_V^1 - g_A^1)\Psi_S \right\} Z_\mu, \qquad (4.8)$$

---

[6]Calculations can be found in refs. [16–18] and their appendices for the simple case of the four-fermion operator (3.8), where composite particles carry the definite quantum numbers of the $SU_L(2)$-gauge symmetry, and their tree-level gauge-couplings to the $SU_L(2)$-gauge bosons can be obtained by the Ward identity associating to the $SU_L(2)$-gauge symmetry in the UV-domain of the symmetric phase.

where i remains as the $SU_L(2)$-isospin index. For the d_R-quark channel, the composite particles made by $u_{Ra} \to d_{Ra}$, the coupling $g_{V,A}^1 \to g_{V,A}^2$ and $(2/3)e \to (-1/3)e$. These massive composite fermions couple to the gauge bosons $W_\mu^\pm = (W_\mu^1 \mp iW_\mu^2)/\sqrt{2}$, $A_\mu = B_\mu \cos\theta_W + W_\mu^3 \sin\theta_W$ and $Z_\mu = -B_\mu \sin\theta_W + W_\mu^3 \cos\theta_W$. The Lagrangian (4.8) shows that the massive spectrum and interacting vertex are vector-like fully preserving the parity symmetry. Namely, each left-handed (right-handed) SM elementary fermion has its counterpart of right-handed (left-handed) composite fermion with the same quantum numbers of the SM chiral gauge symmetries. They form a massive Dirac composite fermion vectorially coupling to the SM gauge bosons.

For the massive composite bosons $SU_L(2)$-doublet $\mathcal{A}^i$ (4.1) for the u_R channel, i.e., the neutral component $\mathcal{A}^1 \sim (\bar{u}_{Ra}u_L^a)$ and charged component $\mathcal{A}^2 \sim (\bar{u}_{Ra}d_L^a)$ of the $U_Y(1)$-hypercharge $Y = -1/2$, the effective Lagrangian reads

$$\mathcal{L} = \sum_i \left[|\mathcal{D}\mathcal{A}^i|^2 + M_\Pi^2 |\mathcal{A}^i|^2 \right],\tag{4.9}$$

where

$$\mathcal{D}\mathcal{A}^i = (\partial_\mu + ig_2\sigma \cdot \mathbf{W}_\mu/2 + ig_1 Y B_\mu)\mathcal{A}^i\tag{4.10}$$

$$= \left[\partial_\mu + i\frac{g_2}{\sqrt{2}}\left(T^+ W_\mu^+ + T^- W_\mu^-\right) + ie \begin{pmatrix} \sin^{-1}2\theta_W Z_\mu & 0 \\ 0 & -\tan^{-1}2\theta_W Z_\mu - A_\mu \end{pmatrix} \right] \mathcal{A}^i$$

and σ is the Pauli matrix in the isospin space. Instead, for the massive composite bosons $SU_L(2)$-doublet $\mathcal{A}^i$ for the d_R channel, i.e., the charged component $\mathcal{A}^1 \sim (\bar{d}_{Ra}u_L^a)$ and neutral component $\mathcal{A}^2 \sim (\bar{d}_{Ra}d_L^a)$ of the $U_Y(1)$-hypercharge $Y = 1/2$, Equation (4.10) becomes

$$\mathcal{D}\mathcal{A}^i = (\partial_\mu + ig_2\sigma \cdot \mathbf{W}_\mu/2 + ig_1 Y B_\mu)\mathcal{A}^i\tag{4.11}$$

$$= \left[\partial_\mu + i\frac{g_2}{\sqrt{2}}\left(T^+ W_\mu^+ + T^- W_\mu^-\right) + ie \begin{pmatrix} \tan^{-1}2\theta_W Z_\mu + A_\mu & 0 \\ 0 & -\sin^{-1}2\theta_W Z_\mu \end{pmatrix} \right] \mathcal{A}^i.$$

The last matrix-terms in eqs. (4.10) and (4.11) respectively show that the isospin components $\mathcal{A}^1 \sim \bar{u}_R u_L$ and $\mathcal{A}^2 \sim \bar{d}_R d_L$ have no electric charge, but the $U_Y(1)$ hypercharge coupling to Z^0. The gauge couplings in the effective Lagrangian (4.8), (4.10) and (4.11) are consistent with SM gauge bosons couplings to the elementary fermions inside the composite particles, see figure 3.

The effective Lagrangian (4.8), (4.10) and (4.11) can be generalized to the lepton sector and lepton-quark sector. Note that in the effective Lagrangian (4.8) and (4.9), we only present the spectra (kinetic terms or propagators) of massive composite particles and their tree-level gauge-coupling to the elementary SM gauge bosons.

To the leading order of the expansion in the powers of the perturbative SM gauge couplings (the tree-level), the interacting vertexes of composite bosons and fermions coupling to SM gauge bosons ($\gamma, W^\pm, Z^0$) are represented by the tree-level Feynman diagrams, see figure 3, which show gauge bosons interacting with one of elementary particles inside
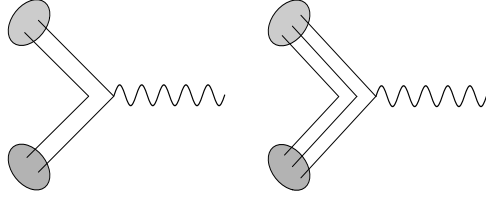
Figure 3. We sketch the vertexes of composite boson (left) and fermion (right) interacting with SM gauge bosons (wave line), and the SM elementary fermion is represented by a solid line. In general, these vertexes should be understood as one-particle-irreducible vertexes of SM gauge bosons interacting with the entire composite particle as an elementary particle. At the lowest tree-level order of perturbative SM gauge couplings, the vertexes can be represented by the sum of possible gauge couplings to an SM elementary particle inside a composite particle. Note that we do not show the vertexes of composite boson (left) interacting with two SM gauge bosons that are present in the effective Lagrangian (4.9).

composite particles. Therefore, this implies that at the tree level, some calculations of Feynman diagrams are similar to those in the SM, however, the fermion spectra and coupling vertexes are vectorlike, see eqs. (4.7) and (4.8). The final results are characterized by the mass scales $M_{\Pi,F}$ (4.4) of composite fermions

$$M_F > M_\Pi \propto \mathcal{E}_\xi, \tag{4.12}$$

in the UV domain and functions of the SM gauge couplings g_1, g_2, g_3 at this mass scale $M_{\Pi,F}$, rather than the electroweak scale $v \approx 239.5\,\text{GeV}$ in the IR domain.

Since the propagators of massive composite particles are obtained from the lowest nontrivial contribution of the strong-coupling expansion [14, 15], it cannot be precluded that there could be the interacting vertexes between massive composite particles, e.g., the Yukawa-type interactions of composite bosons and fermions, stemming from the high-order contributions of the strong-coupling expansion. In this article, we do not attempt to discuss the interacting vertexes among composite particles and their relevance in the UV-domain.

4.2.3 Some discussions on FCNC and anomalies in UV-domain

We attempt to have some discussions on the analogical FCNC processes of the UV effective Lagrangian (4.8) and (4.9) of composite particles in the UV-domain. The composite-fermion case is considered as an example for discussions that apply also to the composite-boson case. Recall that (i) composite fermions Ψ^f are composed by the SM elementary fermions ψ^f in the same family "f"; (ii) the fermion-family "diagonalized" effective Lagrangian (4.8), (4.9) of massive composite particles Ψ^f is obtained from the fermion-family "diagonalized" four-fermion operators (2.10) in the mass eigenstates of the SM elementary fermions ψ^f; (iii) the mass eigenstates of composite fermions coincide with the mass eigenstates of the SM elementary fermions in the scenes that composite fermions are composed by elementary fermions in their mass eigenstates, see section 4.1; (iv) the mass and gauge eigenstates of composite fermions are *identical*, due to the exact conservation of the SM chiral gauge symmetries.

In the representation of mass eigenstates of composite fermions, totally contrary to the IR effective Lagrangian for the SM in the IR domain, see section 3.1 and in particular section 3.1.3, the UV effective Lagrangian (4.8) and (4.9) are realized in the scaling UV-domain of the *symmetric phase*, where the expectational values of two-fermion operators (2.11) $\langle \psi_R^f \bar{\psi}_L^f \rangle \propto m^f \equiv 0, f = 1, 2, 3$, identically vanish. The strong-coupling dynamics that forms massive composite particles in the symmetric phase is totally independent of the SM elementary fermion masses m_f in the symmetry-breaking phase. The SM chiral-gauge symmetries and global fermion-family symmetry are exactly preserved by the strong-coupling dynamics and massive spectrum of composite fermions. More precisely, in the representation of mass eigenstates of composite fermions, the fermion-family number associating to the symmetry $U_L^f(1) \times U_R^f(1)$ $f = 1, 2, 3$ for the composite fermion Ψ^f in each family is exactly conserved. Therefore, any process violating fermion-family number is impossible, namely any $\mathcal{FCNC}$ process is completely prohibited. Here the notation $\mathcal{FCNC}$ refers to the process of changing one *composite* fermion Ψ^f flavor to another *composite* fermion $\Psi^{f'}$ flavor with the same electric charge, which is different from the notion FCNC of the IR effective Lagrangian for the SM elementary fermions in the IR-domain.

However, as perturbatively turning on chiral-gauge-boson interactions to composite fermions, does the interactions between the chiral-gauge-boson $W^{\pm}$ and composite fermions introduce a suppressed 1PI vertex for the $\mathcal{FCNC}$ at loop level, analogous to that of the SM effective Lagrangian in the IR domain? The answer is no, for the reason that the mass and gauge eigenstates of composite fermions are identical, and fermion-family mixing matrices (2.14) do not associate to the interacting vertexes of the $W^{\pm}$ boson and composite fermions (4.8). In conclusion, fermion-family-number violating processes like $\mathcal{FCNC}$ are impossible for the effective Lagrangian (4.8) and (4.9) in the UV-domain. The remained question is how the suppressed 1PI vertexes of the FCNC from the SM $W^{\pm}$-boson loop and CKM-type mixing matrices in the IR-domain is induced, when composite fermions decay into SM elementary fermions, a phase transition occurs from symmetric phase ($m_f = 0$) to symmetry-breaking phase ($m_f \neq 0$). This is deserved to study in another article.

In the SM Lagrangian (4.7) of chiral-gauge symmetries and chiral-gauged fermion spectra, the chiral-gauge anomalies associating to the $SU_L(2) \times U_Y(1)$ chiral-gauge symmetries are canceled, because of the $SU_L(2)$ Lie algebra and the SM fermion content of quarks and leptons in each fermion family, and the non conservation of fermion number $(B - L)$ is given by the instanton contribution. In the effective Lagrangian (4.8) of composite particles, although the gauge symmetries are still chiral, i.e., $SU_L(2) \times U_Y(1)$, the spectra of composite fermions Ψ_D and Ψ_S are vector-likely gauged. As a result, the chiral-gauge anomalies from the left-handed composite fermions are exactly canceled by the anomalies from their right-handed counterparts. In the effective Lagrangian (4.8) of composite fermions, we obtained [16] the non conservation of fermion number $(B - L)$ by considering the mixing anomaly [65].

As the running energy scale μ decreasing, and composite particle's form factor and binding energy vanishing, the composite particles become unstable and dissolve (decay) to their constitutes of SM elementary particles as final states. In the following, we discuss

the decay and annihilation channels of the composite particles into the SM elementary particles, in particular two gauge bosons, as final states.

5 Composite pesudo scalar bosons decay

This section 5 and next section 6 discuss the decays and other relevant processes of composite bosons and fermions interacting with SM gauge bosons described by the effective Lagrangians (4.8) and (4.9) of the effective theory of composite particles in UV-domain. These results provide possible connections with the diboson and other channels in ATLAS and CMS experiments.

5.1 Low-energy QCD pions and their decays

First let us recall the low-energy hadronic physics of mesons (baryons) that are the bound states of two quarks (three quarks) due to the confinement dynamics of the local SU(3)-color gauge theory (QCD). This can be approximately described by the effective low-energy Lagrangian of baryons and mesons, which could be realized in the possible low-energy IR-domain of the QCD theory. On the other hand, asymptotically-free states of quarks and gluons are realized in the high-energy UV-domain of the QCD theory. In both bound states and asymptotically-free states, elementary quarks have the same electroweak couplings to the SM gauge bosons $W^\pm$, Z^0 and γ.

To effectively study the non-perturbative nature of low-energy QCD theory, the global chiral-symmetric Lagrangian (σ-model) was adopted to describe the massless QCD-bound states of elementary u and d quarks: proton $p(uud)$, neutron $n(ddu)$ and pions $\pi^{0,\pm}$(uu,dd,ud). The spontaneous breaking of the $SU_L(2) \times SU_R(2)$ chiral symmetries leads to the massive doublet baryon fields (p, n) and massless triplet pion fields π^k as three Goldstone bosons. The explicit breaking induced by the u and d quark masses leads to massive pion fields π^k and the partial conservation of the axial current (PCAC)

$$\partial^\mu A_\mu^j(x) = m_\pi^2 f_\pi \pi^j(x) \tag{5.1}$$

where the quark doublet $\psi^i = (u, d)$ and the axial current $A_\mu^j(x) = \bar\psi \gamma_\mu \gamma_5 (\sigma^j/2)\psi$. The latter couples to the pion fields $\pi^j(x)$ due to the spontaneous breaking of chiral symmetries, leading to the nontrivial matrix elements between the pion state $|\pi^k(p)\rangle$ and the vacuum

$$\langle 0|A_\mu^j(x)|\pi^k(p)\rangle = ip_\mu f_\pi \delta^{jk} e^{-ipx}, \quad \langle 0|\partial^\mu A_\mu^j(x)|\pi^k(p)\rangle = m_\pi^2 f_\pi \delta^{jk} e^{-ipx}. \tag{5.2}$$

The first matrix element defines the pion decay constant (form factor) f_π, the second matrix element and the mass-shell condition $p^2 = m_\pi^2$ defines the pion mass m_π. The charged pions $\pi^\pm = (\pi^1 \mp i\pi^2)/2 = \bar d\gamma_5 u, \bar u\gamma_5 d$ and neutral pion $\pi^0 = \pi^3/2 = (\bar u\gamma_5 u - \bar d\gamma_5 d)/2$. For the isospin $j, k = 1, 2$ components in eq. (5.1), the first matrix element determines the rate of the decay $\pi^+(\bar ud) \to \mu^+ + \nu_\mu$ and experimental value $f_\pi \approx 93\,\text{MeV}$. In addition, for the isospin $j = k = 3$ component in eq. (5.1) reads

$$\partial^\mu A_\mu^3 = m_\pi^2 f_\pi \pi^0 - \frac{\alpha}{8\pi} \, \epsilon_{\mu\nu\rho\sigma} F^{\mu\nu} F^{\rho\sigma}, \tag{5.3}$$
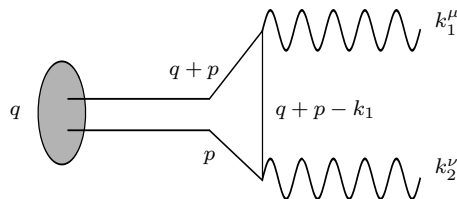
Figure 4. We show the triangle diagram (a quark loop of solid line) of a composite boson (two parallel solid lines associating to a pseudo-scalar vertex γ_5) decaying into the two SM gauge bosons (two wave lines associating to two vector-like vertexes γ_μ and γ_ν).

receiving an axial anomaly in terms of the gauge field (photon) strength F and fine-structure constant α, contributed from the triangle diagram shown in figure 4. This axial anomaly dominates the π^0-decay rate,

$$\Gamma_{\pi^0 \to \gamma\gamma} = \left(\frac{\alpha N_c}{3\pi f_\pi}\right)^2 \frac{m_{\pi^0}^3}{64\pi}, \tag{5.4}$$

in excellent agreement with the experimental value.

5.2 Scalar and pesudo scalar composite bosons

We attempt to study the decays of composite bosons $\mathcal{A}^i$ in the UV-domain, discussed in sections 4.1 and 4.2. For the sake of simplicity, we adopt the first quark family $\psi_L^i = (u, d)_L$ and $\psi_R = u_R, d_R$ for illustrations. For the u-channel, the massive composite boson $\mathcal{A}^i = (\bar{u}_R \psi_L^i)$ (4.1), which is an $SU_L(2)$ doublet and $U_Y(1)$ charged $Y = -1/2$, can expressed in terms of scalar and pseudo scalar fields,

$$\mathcal{A}^i = (\bar{u}_R \psi_L^i) = (1/2) \left[(\bar{u}\psi^i) - (\bar{u}\gamma_5\psi^i)\right]. \tag{5.5}$$

where the form factor $[Z_\Pi^S]^{-1/2}$ is omitted for simplifying notations. There are four components

$$S^0 = \bar{u}u, \quad S^- = \bar{u}d; \qquad \Pi^0 = \bar{u}\gamma_5 u, \quad \Pi^- = \bar{u}\gamma_5 d \tag{5.6}$$

where the isospin index $i = 1, 2$ are relabeled as $i' = 0, \pm$ indicating the neutral or charged component. For the d-channel, by the substitution $u \to d$ in eqs. (5.5) and (5.6), we have

$$\mathcal{A}^i = (\bar{d}_R \psi_L^i) = (1/2) \left[(\bar{d}\psi^i) - (\bar{d}\gamma_5\psi^i)\right],$$
$$S^0 = \bar{d}d, \quad S^+ = \bar{d}u; \qquad \Pi^0 = \bar{d}\gamma_5 d, \quad \Pi^+ = \bar{d}\gamma_5 u. \tag{5.7}$$

The neutral state Π^0 has the contributions from eqs. (5.6) and (5.7) that can be mixed up, but is different from the normal pion $\pi^0 = (\bar{u}u - \bar{d}d)/\sqrt{2}$ in the SU(3) quark model where the minus sign comes from the isospin $\tau^3 = (1, -1)$. The discussions can be generalized to other families including leptons. The second and third families of composite bosons are simply replicated by the replacements $u \to c, t$ and $d \to s, b$. There is no mixing among three families of composite bosons. The gauge interactions at the leading order (tree-level) of gauge couplings (4.10) and (4.11) do not introduce the mixing of composite bosons (5.6) with its counterparts in the second or third family.

These composite bosons $\Pi^{0,\pm}$ (5.6) and (5.7) are bound by the strong-coupling dynamics in the UV domain, differently from the QCD-bound mesons. They have the same *chiral-invariant* mass M_Π (4.4). Instead the three pion fields $\pi^{0,\pm}$ have the *chiral-variant* mass m_π. The vectorial and axial currents associating to the global $SU_L(2) \times U_Y(1)$ chiral symmetries are exactly conserved because these chiral symmetries are preserved, apart from the chiral gauge anomaly (axial anomaly). Instead the axial current associating to the global chiral symmetries of the effective low-energy Lagrangian of the QCD-bound states are partially conserved because of spontaneous and explicit chiral-symmetry-breaking (PCAC). However, the massive pseudo scalar fields $\Pi^{0,\pm}$ (5.6), (5.7) and the QCD pion fields $\pi^{0,\pm}$ have the same quantum numbers of the SM symmetries. Moreover, we shall show the pseudo-scalar fields $\Pi^{0,\pm}$ decay into SM elementray particles, in particular the Π^0-decay into two SM gauge bosons, analogously to the decay $\pi^0 \to \gamma\gamma$, attributing to the axial anomaly (5.4).

5.3 Composite particle Π^0 decay into two SM gauge bosons

5.3.1 Π^0 decay into two photons

Suppose the vacuum state is $|\mathbf{0}\rangle$ in the UV domain, the composite-boson momentum state $|\mathcal{A}^i(q)\rangle$ on the mass shell can be defined by the field operator $\mathcal{A}^i(q)$ or $\mathcal{A}^i(x)$ as follow

$$|\mathcal{A}^i(q)\rangle \equiv \frac{1}{F_\Pi}\mathcal{A}^{i\dagger}(q)|\mathbf{0}\rangle = \frac{1}{F_\Pi}\int d^4x e^{-iqx}\mathcal{A}^{i\dagger}(x)|\mathbf{0}\rangle, \tag{5.8}$$

with the normalization

$$\langle \mathcal{A}^i(q)|\mathcal{A}^{i'}(q')\rangle = \delta^{ii'}(2\pi)^4\delta^4(q-q'), \tag{5.9}$$

or equivalently

$$\langle \mathbf{0}|\mathcal{A}^i(x)|\mathcal{A}^{i'}(q)\rangle = F_\Pi\delta^{ii'}e^{iqx}, \tag{5.10}$$

where $F_\Pi^{-1} = F_\Pi^{-1}(q^2)$ relates to the form factor $[Z_\Pi^S]^{-1/2}$ (4.1), as discussed in section 4. As will be seen soon, F_Π is in fact the composite-boson decay constant. From eq. (5.10), the matrix element reads

$$\langle \mathbf{0}|\partial^\mu\mathcal{A}^i(x)|\mathcal{A}^{i'}(q)\rangle = iq^\mu F_\Pi\delta^{ii'}e^{iqx}. \tag{5.11}$$

The effective Lagrangian (4.9) gives the equation of motion and the mass-shell condition $q^2 = M_\Pi^2$ of the composite boson $\mathcal{A}^i(x)$. From eq. (5.11), we have

$$\langle \mathbf{0}|(\partial^\mu)^2\mathcal{A}^i(x)|\mathcal{A}^{i'}(q)\rangle = M_\Pi^2 F_\Pi\delta^{ii'}e^{iqx}. \tag{5.12}$$

The matrix element (5.10) relates to the composite-boson propagator,

$$\langle \mathbf{0}|\mathcal{A}^i(0)|\mathcal{A}^{i'}(q)\rangle = \frac{1}{F_\Pi}\int d^4x\langle \mathbf{0}|\mathcal{A}^i(0)\mathcal{A}^{i'\dagger}(x)|\mathbf{0}\rangle e^{-iqx} = \frac{\delta^{ii'}F_\Pi^{-1}(q^2)}{q^2 - M_\Pi^2}. \tag{5.13}$$

The matrix element of composite particle Π^0 in eqs. (5.6) and (5.7) reads,

$$\langle f(p')|\Pi^0(0)|f(p)\rangle = \frac{g_{\Pi^0}}{-q^2 + M_\Pi^2}\bar{u}_f(p')\gamma_5 u_f(p), \quad q = p' - p \tag{5.14}$$

– 28 –

where the $g_{\Pi^0} = g_{\Pi^0}(q^2)$ is the Π^0-coupling to its constituent fermions $f = u, d$ quarks of mass m_f and wave function u_f. Actually, the coupling $g_{\Pi^0}(q^2)$ is the 1PI vertex function of composite particle Π^0 and its constituent fermions and we parametrize it by the form factor $F_\Pi^{-1}(q^2)$ and constituent mass m_f

$$g_{\Pi^0}(q^2) = m_f F_\Pi^{-1}(q^2), \tag{5.15}$$

and g_{Π^0} is finite as $m_f \to 0$, see for example [66]. These definitions and equations apply also for scalar composite bosons S^i and pseudo scalar composite bosons Π^i, see eqs. (5.6) and (5.7).

We are in the position of discussing the rate of the neutral Π^0 decay into two SM gauge bosons, i.e., diboson channels:

$$\Pi^0 \to G + G', \tag{5.16}$$

where G and G' represent the SM gauge bosons $W^\pm, Z^0$ and γ. The amplitude of the decay (5.16) is defined by the matrix element

$$\mathcal{F}(q^2)\Big|_{q^2 \to M_{\Pi^0}^2} = \epsilon_1^\mu(k_1)\epsilon_2^\nu(k_2)T_{\mu\nu}(k_1, k_2, q)\Big|_{q^2 \to M_{\Pi^0}^2}, \quad q = k_1 + k_2 \tag{5.17}$$

and

$$T_{\mu\nu}(k_1, k_2, q) = (q^2 - M_{\Pi^0}^2)(gg') \int d^4x d^4y e^{ik_1 x + ik_2 y}\langle \mathbf{0}|T(J_\mu(z)J_\nu'(y)\Pi^0(0))|\mathbf{0}\rangle, \tag{5.18}$$

where $k_{1,2}$ and $\epsilon_{1,2}$ are four momenta and polarizations of the SM gauge bosons G and G', and $J_\mu(z)$ $[J_\nu'(y)]$ is fermion current coupling g $[g']$ to the SM gauge boson G $[G']$. The amplitude $T_{\mu\nu}(k_1, k_2, q)$ has the symmetry $(k_1, \mu) \leftrightarrow (k_2, \nu)$.

The lowest one-loop contribution to the vertex function (5.18) is represented by the triangle Feynman diagram, see figure 4. Considering eqs. (5.14) and (5.15), the Π^0-decay amplitude $T_{\mu\nu}$ (5.18) computed at this one-loop level is given by

$$T_{\mu\nu}(k_1, k_2, q) = T_{\mu\nu}^{(1)}(k_1, k_2, q, m_f) + T_{\nu\mu}^{(2)}(k_2, k_1, q, m_f), \tag{5.19}$$

$$T_{\mu\nu}^{(1)}(k_1, k_2, q, m_f) = -(gg')N_c m_f F_\Pi^{-1}(q^2) \times$$

$$\times \int \frac{d^4p}{(2\pi)^4} \frac{\mathrm{tr}[(\not{q}+\not{p}-\not{k}_1+m_f)\Gamma_\mu(\not{q}+\not{p}+m_f)\gamma_5(\not{p}+m_f)\Gamma_\nu']}{[(q+p-k_1)^2 - m_f^2][(q+p)^2 - m_f^2](p^2 - m_f^2)}, \tag{5.20}$$

where the coupling vertexes $g\Gamma_\mu$ and $g'\Gamma_\nu'$ to the SM gauge bosons G and G' are given by the SM Lagrangian (4.8), and the trace "tr" is over the spinor space. Equation (5.20) is not well-defined because of the linear divergence of the momentum integral. Introducing the Pauli-Villars mass $\mathcal{M}$ that plays the role of the UV cutoff Λ, we adopt the Pauli-Villars regularization,

$$T_{\mu\nu}^{(1)}(k_1, k_2, q, m_f) \to T_{\mu\nu}^{(1)}(k_1, k_2, q, m_f) - T_{\mu\nu}^{(1)}(k_1, k_2, q, \mathcal{M}) \tag{5.21}$$

to make the momentum integral to be finite and well-defined. Note that the Pauli-Villas regularization $\mathcal{M}$ explicitly breaks chiral gauge symmetries of effective Lagrangian.

For the process $\Pi^0 \to \gamma + \gamma$, $g = g' = e\, Q^i$, $\Gamma_\mu = \gamma_\mu$ and $\Gamma'_\nu = \gamma_\nu$ in eq. (5.20). The $J_\mu(z)$ and $J'_\nu(y)$ in eq. (5.18) are vector-like and conserved fermion currents coupling with two on-shell photons k_1 and k_2. The trace in the numerator of eq. (5.20) is equal to $4im_f\epsilon_{\mu\nu\rho\sigma}k_1^\sigma k_2^\rho$. With the on-shell conditions $k_1^2 = 0$, $k_2^2 = 0$ and $2k_1 \cdot k_2 = q^2$, the two contributions (5.19) to the amplitude (5.17) of Π^0 decaying into two photons is given by

$$
\mathcal{F}(q^2)\Big|_{q^2 \to M_{\Pi^0}^2} = \frac{(gg')N_c}{2\pi^2 F_\Pi}\epsilon_{\mu\nu\rho\sigma}\epsilon_1^\mu\epsilon_2^\nu k_1^\rho k_2^\sigma
$$
$$
\times \int_0^1 dx \int_0^{1-x} dy \left[\frac{\mathcal{M}^2}{\mathcal{M}^2 - xyq^2} - \frac{m_f^2}{m_f^2 - xyq^2}\right]_{q^2 \to M_{\Pi^0}^2} \tag{5.22}
$$
$$
= \frac{(gg')N_c}{4\pi^2 F_\Pi}\epsilon_{\mu\nu\rho\sigma}\epsilon_1^\mu\epsilon_2^\nu k_1^\rho k_2^\sigma. \tag{5.23}
$$

The second term in eq. (5.22) is suppressed for $M_{\Pi^0} \gg m_f$ and the first term for $\mathcal{M} \to \infty$ leading to the final result (5.23). The result is just the axial anomaly of the triangle Feynman diagram (figure 4) with one axial vertex "γ_5" and two vector-like (AVV) vertexes "$\gamma_5\gamma_\mu\gamma_\nu$". This axial-anomaly result (5.23) is due to the regularization that does not preserve chiral gauge symmetries of effective Lagrangian, and it is independent of high-order contributions, constituent fermion mass m_f and UV cutoff $\mathcal{M}$. Equation (5.23) shows that the F_Π value at $q^2 = M_{\Pi^0}^2$ is the Π^0-decay constant. For the first quark family, there are two Π^0 channels (5.6) and (5.7) with $Q_i = (2/3, -1/3)$, i.e., $g^2 = e^2(4/9, 1/9)$. The total amplitude of $\Pi^0 \to \gamma + \gamma$ reads,

$$
\mathcal{F}(q^2)\Big|_{q^2 \to M_{\Pi^0}^2}^{\Pi^0 \to \gamma+\gamma} = \sum_i (Q^i)^2 \frac{e^2 N_c}{4\pi^2 F_\Pi}\epsilon_{\mu\nu\rho\sigma}\epsilon_1^\mu\epsilon_2^\nu k_1^\rho k_2^\sigma = \left(\frac{5}{9}\right)\mathcal{F} \tag{5.24}
$$
$$
\mathcal{F} \equiv \frac{e^2 N_c}{4\pi^2 F_\Pi}\epsilon_{\mu\nu\rho\sigma}\epsilon_1^\mu\epsilon_2^\nu k_1^\rho k_2^\sigma. \tag{5.25}
$$

The amplitude (5.24) should be multiplied by a factor $N_c = 3$, if we consider three quark families.

It needs some more clarifications on the amplitude (5.24). Both the composite pseudo-scalar boson Π^0 and the composite scalar Higgs boson H decay into the two-photon state, however these two channels are not mixed. They have different parities, masses (invariant masses) and decay constants. The former composed by the strong-coupling dynamics in the UV-domain decay into two photons via the pseudo-scalar coupling (see figure 4) to the loop of u and d quarks. Whereas the latter composed by the NJL-dynamics in the IR-domain via the scalar coupling $\bar{t}tH$ (4.7) to a top-quark loop. In the LHC pp collision, the first family of composite particles made of u and d quarks are more probably produced, compared with other families of composite particles that are produced by small SM gauge interacting vertexes.

5.3.2 Π^0 decay into $\gamma + Z^0$, $W^+ + W^-$ and $Z^0 + Z^0$

Let us study other possible decay channels $\Pi^0 \to \gamma + Z^0$, $\Pi^0 \to W^+ + W^-$ and $\Pi^0 \to Z^0 + Z^0$. Suppose that the pseudo scalar composite field $\Pi^0(x)$ is heavy and its mass M_{Π^0}

is much larger than the $W^\pm$ and Z^0 masses, the intermediate gauge bosons $W^\pm$ and Z^0 are considered to be approximately massless, $k_1^2 \approx 0$, $k_2^2 \approx 0$ and $2k_1 \cdot k_2 \approx q^2$. In addition, the coupling-vertexes $g\Gamma_\mu$ and $g'\Gamma'_\nu$ in eq. (5.20) are given in the SM Lagrangian (4.7), they contain both axial and vector-like vertexes. We consider the vector-like vertexes so that the triangle Feynman diagram (figure 4) and the amplitude (5.18) has the AVV structure, whose nontrivial axial-anomaly amplitude can be compared with the amplitude (5.24) of the channel $\Pi^0 \to \gamma + \gamma$. As a result, for the process $\Pi^0 \to \gamma + Z^0$, the couplings $g = eQ^i$ and $g' = g_2 g_V^i/(2\cos\theta_W)$, we obtain from eq. (5.23) the amplitude,

$$
\begin{aligned}
\mathcal{F}(q^2)\Big|_{q^2 \to M_{\Pi^0}^2}^{\Pi^0 \to \gamma + Z^0} &= \frac{1}{\sin 2\theta_W} \sum_i (Q^i g_V^i) \mathcal{F} \\
&= \frac{1}{\sin 2\theta_W} \left(\frac{1}{2} - \frac{5}{9} \sin\theta_W^2 \right) \mathcal{F}.
\end{aligned}
\tag{5.26}
$$

For the process $\Pi^0 \to W^+ + W^-$, the couplings $g = g' = g_2/(2\sqrt{2})$ and we obtain from eq. (5.23) the amplitude,

$$
\mathcal{F}(q^2)\Big|_{q^2 \to M_{\Pi^0}^2}^{\Pi^0 \to W^+ + W^-} = \frac{1}{8\sin^2\theta_W} \sum_i \mathcal{F} = \frac{1}{8\sin^2\theta_W} \mathcal{F},
\tag{5.27}
$$

where the sum over isospin "i" gives one in this case, see eq. (4.7). For the process $\Pi^0 \to Z^0 + Z^0$, the couplings $g = g' = g_2 g_V^i/(2\cos\theta_W)$ and we obtain from eq. (5.23) the amplitude,

$$
\begin{aligned}
\mathcal{F}(q^2)\Big|_{q^2 \to M_{\Pi^0}^2}^{\Pi^0 \to Z^0 + Z^0} &= \frac{1}{\sin^2 2\theta_W} \sum_i (g_V^i)^2 \mathcal{F} \\
&= \frac{1/2 - \sin^2\theta_W + (5/9)\sin^4\theta_W}{\sin^2 2\theta_W} \mathcal{F}.
\end{aligned}
\tag{5.28}
$$

Their differences from the two-photon amplitude (5.24) are only attributed to the different eletroweak couplings of the SM (4.7).

5.4 Ratios of different channels of Π^0 decay into two SM gauge bosons

The numerical rate of the neutral $\Pi^0(q)$ decay (5.16) at the mass shell ($q^2 = M_{\Pi^0}^2$) is given by integrating the squared amplitude (5.17) over the phase space of two gauge bosons,

$$
\begin{aligned}
\Gamma_{\Pi^0 \to G + G'} &= \frac{1}{2M_{\Pi^0}} \sum_{\epsilon_1, \epsilon_2} \int \frac{d^3k_1 d^3k_2}{4(2\pi)^6 \omega_1 \omega_2} \Big| \mathcal{F}(q^2) \Big|_{\Pi^0 \to G + G'}^2 \\
&\quad \times (2\pi)^4 \delta^4(q - k_1 - k_2) \Big|_{q^2 = M_\Pi^2} \\
&= \mathcal{C}_{\Pi^0 \to G + G'} \, \Gamma,
\end{aligned}
\tag{5.29}
$$

$$
\Gamma \equiv \left(\frac{\alpha N_c}{3\pi F_\Pi} \right)^2 \frac{M_{\Pi^0}^3}{64\pi},
\tag{5.30}
$$

where the mass M_{Π^0} and decay constant F_Π of the composite boson Π^0 are totally unknown, while the coefficients $\mathcal{C}_{\Pi^0 \to G + G'}$ are completely determined from eqs. (5.24), (5.26), (5.27)

and (5.28) in terms of SM gauge couplings. Note that the decay rates (5.29) depend on the Π^0 mass M_{Π^0} and decay constant F_Π determined by the strong-coupling dynamics, analogously to the pion mass m_π and decay constant f_π determined by the QCD dynamics.

In the rest frame of the composite meson Π^0, the final states of two body decay follow the energy-momentum conservations $\mathbf{p}_1 = -\mathbf{p}_2, |\mathbf{p}_1| = |\mathbf{p}_2|$ and have the invariant mass $\mathcal{M}_{\text{inv}} = M_{\Pi^0}$. The rates of the composite meson Π^0 decaying into two SM gauge bosons G and G' are given by eq. (5.29), we then obtain the rates of diboson channel decay (5.16):

$$\Gamma_{\Pi^0 \to \gamma + \gamma} = \left(\frac{5}{9}\right)^2 \Gamma, \tag{5.31}$$

$$\Gamma_{\Pi^0 \to \gamma + Z^0} = \frac{1}{\sin^2 2\theta_W} \left(\frac{1}{2} - \frac{5}{9}\sin^2\theta_W\right)^2 \Gamma, \tag{5.32}$$

$$\Gamma_{\Pi^0 \to W^+ + W^-} = \left(\frac{1}{8\sin^2\theta_W}\right)^2 \Gamma, \tag{5.33}$$

$$\Gamma_{\Pi^0 \to Z^0 + Z^0} = \left(\frac{1/2 - \sin^2\theta_W + (5/9)\sin^4\theta_W}{\sin^2 2\theta_W}\right)^2 \Gamma. \tag{5.34}$$

The diphoton channel (5.31) is expected to have the largest branching ratio, analogously to the QCD pion decay $\pi^0 \to \gamma\gamma$. Suppose that the possible resonance of the diphoton channel (5.31) of the invariant mass $\mathcal{M}_{\gamma\gamma}$ is observed in high-energy experiments, it implies that the composite meson mass $M_{\Pi^0} \gtrsim \mathcal{M}_{\gamma\gamma}$, since there are other decay channels (5.32), (5.33), (5.34) into two gauge bosons of γZ^0, W^+W^- and Z^0Z^0. The channel γZ^0 corresponds to the final states of a photon and two leptons or a "fat" jet of two quarks. The channels W^+W^- and Z^0Z^0 correspond to the final states of (i) two "fat" jets of four quarks for W and Z hadronic decays or (ii) four leptons for W and Z leptonic decay, or a "fat" jet and two leptons in the combination of cases (i) and (ii).

For the reasons that the properties of composite particles, e.g., form-factors and masses (or the binding-energy depth) due to the strong-coupling dynamics, are unknown, we have not been able to calculate the total rate $\Gamma_{\Pi^0}^{\text{total}}$ and width of the composite boson Π^0 that decays into the final states of the SM elementary particles including the channel of two gauge bosons or two fermions.[7] Nevertheless, at the leading order (tree-level) of gauge interactions, we are able to calculate the rates $\Gamma_{\Pi^0 \to \gamma\gamma, \gamma Z, \cdots}$ (5.29) of the composite boson Π^0 decaying into two gauge bosons as diboson final states,

$$\Pi^0 \to \gamma\gamma, \gamma Z^0, W^+W^-, Z^0Z^0, \cdots. \tag{5.35}$$

These diboson channels (5.35) are expected to be the most energetically favorable and largest branching ratio,

$$B_{\Pi^0 \to \gamma\gamma, \gamma Z^0, W^+W^-, Z^0Z^0} = \frac{\Gamma_{\Pi^0 \to \gamma\gamma, \gamma Z^0, W^+W^-, Z^0Z^0}}{\Gamma_{\Pi^0}^{\text{total}}}. \tag{5.36}$$

Moreover, in high-energy experiments, the diboson final state and its kinematics might be more easily identified than the final state of two fermions (quarks or two jets) due to the background of the QCD dynamics.

---

[7]In ref. [20], we have some discussions of composite boson decaying into the final state of two quarks.

The total decay rate and width of the composite boson, as well as the branching ratios of decay channels, are very important for the collider phenomenology of the composite boson. However, the following ratios of the branching ratios (5.36) for different decay channels (5.35), "relative branching ratio"

$$\frac{\Gamma_{\Pi^0 \to \gamma\gamma, \gamma Z^0, W^+W^-, Z^0Z^0}}{\Gamma_{\Pi^0 \to \gamma\gamma}} = \frac{B_{\Pi^0 \to \gamma\gamma, \gamma Z^0, W^+W^-, Z^0Z^0}}{B_{\Pi^0 \to \gamma\gamma}} = \frac{\Gamma_{\Pi^0 \to \gamma\gamma, \gamma Z^0, W^+W^-, Z^0Z^0}/\Gamma_{\Pi^0}^{\text{total}}}{\Gamma_{\Pi^0 \to \gamma\gamma}/\Gamma_{\Pi^0}^{\text{total}}},$$
(5.37)

depend only on the SM gauge couplings g and g' at the energy scale M_Π, given by the effective Lagrangian (4.8). Following these discussions and using eqs. (5.31)–(5.34), we can approximately estimate the decay-rate ratios (5.37)

$$\Gamma_{\Pi^0 \to \gamma Z^0}/\Gamma_{\Pi^0 \to \gamma\gamma} = \frac{\left(9/10 - \sin^2\theta_W\right)^2}{\sin^2 2\theta_W} \approx 0.63,$$

$$\Gamma_{\Pi^0 \to W^+W^-}/\Gamma_{\Pi^0 \to \gamma\gamma} \approx \left(\frac{9}{40\sin^2\theta_W}\right)^2 \approx 0.96,$$

$$\Gamma_{\Pi^0 \to Z^0Z^0}/\Gamma_{\Pi^0 \to \gamma\gamma} = \left(\frac{(9/10) - (9/5)\sin^2\theta_W + \sin^4\theta_W}{\sin^2 2\theta_W}\right)^2 \approx 0.58, \quad (5.38)$$

where the value $\sin^2\theta_W \approx 0.23$ is approximately adopted to obtain numbers. These relations provide a possibility to verify the validity of such an effective theory of composite particles, if the resonance of diphoton channel and other diboson channels are also observed and measured in high-energy experiments, for instance the on-going ATLAS and CMS experiments in the LHC pp collisions.

It is also possible that the composite boson Π^0 decays into the dijet final state of two quarks which was already discussed in refs. [20, 21]. Suppose that the neutral composite meson Π^0 is produced by pp collisions at the LHC, its resonance location $\mathcal{M}_{\text{all channels}} = M_{\Pi^0}$, and the rate of each decay channel depends on the values of the mass M_{Π^0}, decay constant F_Π and SM gauge couplings at these scales. Which channel is more relevant for detections, depending not only on its theoretical branching ratio in principle, but also on its experimental measurement in practice.

The same analysis and discussion can be generalized to the decay rates of neutral composite bosons Π^0 made of charged lepton and/or neutrino pair (4.5) in the lepton channel. Their decay constants and masses should be approximately at the same scale of the Π^0 decay constant F_Π and mass M_{Π^0}. Their decay rates can be obtained by eqs. (5.24)–(5.30) for $N_c = 1$, couplings Q^i and g_V^i of the lepton sector in the SM Lagrangian (4.7). As an example for the two-photon final state, the rate should be $(5/9)^2 N_c^2 = 25/9$ time smaller than the rate (5.31) of the quark channel. However, the ratios of branching ratios for different diboson channels are similar to eq. (5.38), but modified accordingly to the leptonic Q^i and g_V^i values. Beside, in the LHC pp collision, the production probability of leptonic composite bosons is smaller than hadronic one, due to the leptonic production rate is proportional to the small fine-structure constant α.

– 33 –

5.5 $\Pi^\pm$ and other composite boson decays

Equations (5.1) and (5.2) of the PCAC are not applicable for the charged composite bosons $\Pi^\pm$ decay. Therefore, we cannot use the analogy of the QCD charged pion $\pi^\pm$ decays obtain the rates of $\Pi^\pm$ decay to either two quarks (jets) or two leptons,

$$\Pi^+ \to t + b, \cdots; \tau^+ + \nu_\tau, \cdots, \tag{5.39}$$

and charge-conjugated processes. In the quark case, the composite bosons $\Pi^\pm$ are made of quarks (4.1), and in the lepton case the composite bosons $\Pi^\pm$ are made of leptons (4.5). Nevertheless, it is expected that the $\Pi^\pm$-decay channel to the heaviest fermions, top quark or tau lepton, should be most favorable. Suppose that the charged composite meson $\Pi^\pm$ is produced by pp collisions at the LHC, its resonance locates at the invariant mass $\mathcal{M}_{qq} \approx M_{\Pi^\pm}$ of the dijet final state or other possible final states produced by two quarks (two jets). Whereas the charged lepton channel implies the final state of $\tau^\pm$ lepton of energy $\sim M_{\Pi^\pm}/2$ and missing energy carried away by ν_τ-neutrino.

In eqs. (5.6) and (5.7), the scalar bosons form composite quarkonium states $\bar{u}u$ and $\bar{d}d$ that carry the same quantum numbers of QCD quarknium states, however, have much larger masses $\sim M_{\Pi^0}$. It is expected that apart from different kinematic threshold, these composite quarkonium states in principle undergo all decay channels of QCD quarkonium states. Recall that the direct decays of composite bosons $\Pi^\pm$ and quarkonium states into dijets or dilepton without an intermediate state were preliminarily discussed [20, 21]. On the basis of the SM chiral gauge symmetries and vector-like composite fermion content, there are also other possible final decay channels, analogously to those studied in the effective theory of QCD at low energies. These will be issues in future studies.

6 Composite fermion decay and annihilation channels

In this section 6, we turn to discussions of decay and annihilation channels of composite fermions, see section 4.1, on the basis of the effective Lagrangian (4.8) of their kinetic terms and interactions to SM gauge bosons. We show the peculiar characteristics of composite fermions decay. It could be a possibility and possible criterion for the experimental verification or falsification of the effective theory of composite particles in the UV-domain of strong four-fermion couplings.

6.1 Composite fermions decay

6.1.1 Decay into two gauge bosons and a quark

For the sake of simplicity, we adopt the first quark family (4.1)–(4.3) to discuss the decay of composite Dirac fermions, and discussions can be generalized to other families including leptons. The composite Dirac fermions Ψ_D (4.3) should be more massive than their constituents of composite boson $\mathcal{A}^i$ (4.1), i.e., $M_F > M_\Pi^{0,\pm}$. They decay into the SM elementary particles via the intermediate composite-boson states Π^0 (neutral decay channel) or $\Pi^\pm$ (charged decay channel) or quarkonium states in eqs. (5.6) and (5.7). Suppose that at the present energy of pp collisions at the LHC, composite Dirac fermions produced are

non-relativistic particles, and we consider them to be approximately at rest in the CM frame of pp collision. The neutral decay channels are, see figure 5, for the u-quark channel

$$\Psi_D \to \Pi^0 + [\bar{u}_L, u_R] \to (\gamma\gamma, \gamma Z^0, W^+W^-, Z^0Z^0) + \text{a jet}, \qquad (6.1)$$

and the d-quark channel given by $u \to d$. This indicates that a composite Dirac fermion Ψ_D decays into a composite meson Π^0 and a fundamental Dirac fermion, u-quark $[\bar{u}_L, u_R]$ or d-quark $[\bar{d}_L, d_R]$. The latter is an ultra-relativistic quark, $E_f \approx |\mathbf{p}_f|$, ending as a jet in the final states. And the former is a composite meson, $E_{\Pi^0} = (\mathbf{p}_{\Pi^0}^2 + M_{\Pi^0}^2)^{1/2}$, appearing as an intermediate and metastable state for a short time $\sim 1/M_{\Pi^0}$ then decays into two photons of the energy $E_\gamma = |\mathbf{p}_\gamma|$ or other diboson channels (5.35) of two SM gauge bosons G and G'. In the CM frame of the pp collision, the composite fermion is approximately at rest, and decays into a quark (jet) and a composite boson moving apart in opposite directions $(\mathbf{p}_f = -\mathbf{p}_{\Pi^0})$. The kinematic distribution of final states is described by the invariant mass $\mathcal{M}_{\text{inv}} \approx M_F$,

$$
\begin{aligned}
M_F &= E_f + E_{\Pi^0} \approx |\mathbf{p}_{\Pi^0}| + (\mathbf{p}_{\Pi^0}^2 + M_{\Pi^0}^2)^{1/2}, \\
\mathbf{p}_f &= -\mathbf{p}_{\Pi^0} = -(\mathbf{p}_{\gamma_1} + \mathbf{p}_{\gamma_2}) \\
|\mathbf{p}_{\Pi^0}| &\approx \left[|\mathbf{p}_{\gamma_1}|^2 + |\mathbf{p}_{\gamma_1}|^2 + 2|\mathbf{p}_{\gamma_1}||\mathbf{p}_{\gamma_2}|\cos\theta_{\gamma_1\gamma_2} \right]^{1/2}, \qquad (6.2)
\end{aligned}
$$

where $\theta_{\gamma_1\gamma_2}$ is the angle between the momenta $\mathbf{p}_{\gamma_1}$ and $\mathbf{p}_{\gamma_2}$ of two photons or other diboson states (6.1). The rate $\Gamma_{\Psi_D \to GG'+\text{jet}}$ of composite fermion decay (6.1) should be the product of Π_0-decay rate $\Gamma_{\Pi_{\Pi^0} \to GG'}$ (5.31)–(5.34) and the rate $\Gamma_{\Psi_D \to \Pi^0 + \text{a quark}}$ of Ψ_D decaying into a quark and Π_0, namely

$$\Gamma_{\Psi_D \to GG'+\text{a quark}} \propto \quad \Gamma_{\Psi_D \to \Pi^0 + \text{a quark}} \times \Gamma_{\Pi_{\Pi^0} \to GG'}. \qquad (6.3)$$

This implies the ratios:

$$
\begin{aligned}
\Gamma_{\Psi_D \to \gamma Z^0 + \text{a quark}}/\Gamma_{\Psi_D \to \gamma\gamma + \text{a quark}} &\propto \Gamma_{\Pi^0 \to \gamma Z^0}/\Gamma_{\Pi^0 \to \gamma\gamma}, \\
\Gamma_{\Psi_D \to W^+W^- + \text{a quark}}/\Gamma_{\Psi_D \to \gamma\gamma + \text{a quark}} &\propto \Gamma_{\Pi^0 \to W^+W^-}/\Gamma_{\Pi^0 \to \gamma\gamma}, \\
\Gamma_{\Psi_D \to Z^0Z^0 + \text{a quark}}/\Gamma_{\Psi_D \to \gamma\gamma + \text{a quark}} &\propto \Gamma_{\Pi^0 \to Z^0Z^0}/\Gamma_{\Pi^0 \to \gamma\gamma}. \qquad (6.4)
\end{aligned}
$$

are similar to the ratios (5.38). If the bosonic resonance (5.35) is observed and its invariant mass is determined, the resonance of composite fermion decay (6.1) could possibly be identified by measuring such a peculiar final-state kinematics (6.2) of a single jet and two photons or other diboson states G and G'.

6.1.2 Decay into two gauge bosons and a lepton

Due to the four-fermion interaction of quark-lepton sector, see eq. (2.18) and section 4.1.3, the composite fermions (4.6) composed by a hadronic composite boson and a lepton are also formed in the UV-domain. We generalize the analysis and discussion in the previous section 6.1.1 to the decay of composite fermion (4.6) composed by a hadronic composite
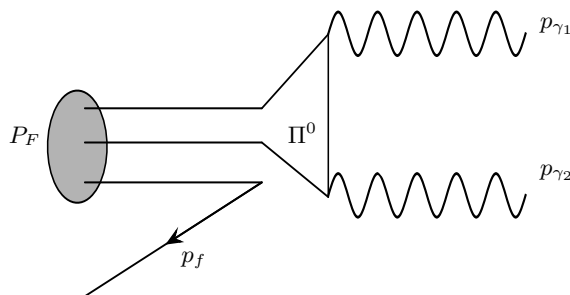
Figure 5. We show the diagram of a composite fermion (three parallel solid lines) decaying to an SM elementary quark or lepton (the solid line with an arrow) and a composite boson, the latter decays into two SM gauge bosons (wave lines), see figure 4. The composite boson Π^0 is an intermediate state. p_f represents the energy momentum of quark or lepton. p_{γ_1} and p_{γ_2} represent the energy momentum of two photons or two gauge bosons G and G'. The composite fermion is heavier than composite boson Π^0, $M_F > M_{\Pi^0}$, and the energy-momentum of composite fermion $E_F = M_F$ at its rest frame ($\mathbf{P}_F = 0$), as described in eq. (6.2).

boson Π^0 and a charged lepton (or a neutrino). The decay process is also represented by figure 5. For the e-lepton channel,

$$\Psi_D \to \Pi^0 + [\bar{e}_L, e_R] \to (\gamma\gamma, \gamma Z^0, W^+W^-, Z^0Z^0) + \text{an electron}, \qquad (6.5)$$

and the ν_e-lepton channel is given by $e \to \nu$. This indicates that a composite Dirac fermion Ψ_D (4.6) decays into a composite meson Π^0 and a fundamental Dirac fermion, a charged lepton $\ell = [\bar{\ell}_L, \ell_R]$ or a neutrino ν_ℓ. The latter is an ultra-relativistic lepton. The kinematic threshold and distribution are the same as the one (6.1) in pure hadronic channel (6.2). However, the neutrino in the final states carries away mixing energy and momentum. The rate $\Gamma_{\Psi_D \to GG'+\text{a lepton}}$ of composite fermion decay (6.5) should be the product of Π_0-decay rate $\Gamma_{\Pi^0 \to GG'}$ (5.31)–(5.34) and the rate $\Gamma_{\Psi_D \to \Pi^0+\text{a lepton}}$ of Ψ_D decaying into a lepton and Π_0, namely

$$\Gamma_{\Psi_D \to GG'+\text{a lepton}} \propto \quad \Gamma_{\Psi_D \to \Pi^0+\text{a lepton}} \times \Gamma_{\Pi^0 \to GG'}. \qquad (6.6)$$

This implies the ratios:

$$\Gamma_{\Psi_D \to \gamma Z^0+\text{a lepton}}/\Gamma_{\Psi_D \to \gamma\gamma+\text{a lepton}} \propto \Gamma_{\Pi^0 \to \gamma Z^0}/\Gamma_{\Pi^0 \to \gamma\gamma},$$
$$\Gamma_{\Psi_D \to W^+W^-+\text{a lepton}}/\Gamma_{\Psi_D \to \gamma\gamma+\text{a lepton}} \propto \Gamma_{\Pi^0 \to W^+W^-}/\Gamma_{\Pi^0 \to \gamma\gamma},$$
$$\Gamma_{\Psi_D \to Z^0 Z^0+\text{a lepton}}/\Gamma_{\Psi_D \to \gamma\gamma+\text{a lepton}} \propto \Gamma_{\Pi^0 \to Z^0 Z^0}/\Gamma_{\Pi^0 \to \gamma\gamma}. \qquad (6.7)$$

are similar to the ratios (5.38).

The decay processes (6.1) and (6.5) discussed in this section show the peculiar characteristics of the effective theory of composite bosons and fermions in the UV-domain of strong four-fermion couplings. These processes are relevant to and can be checked by the on-going high-energy experiments in the LHC pp collision.

– 36 –

6.1.3 Other channels of composite fermion decay

In addition, the decay channels of composite fermions via the intermediate meson state of charged composite bosons $\Pi^{\pm}$ (5.39) read

$$\Psi_D \to \Pi^+ + [\bar{u}_L, d_R], \tag{6.8}$$

and its charge conjugate. The Weyl fields $[\bar{u}_L, d_R]$ do not form a Dirac fermion of u- or d-quark, but pick up u_R and $\bar{d}_L$ quarks from the vacuum, and end as u and d-quark (jets) in final states. On the other hand, the charged composite mesons $\Pi^{\pm}$, see eqs. (5.6) and (5.7), most probably decay into two quarks (5.39). Therefore, the most probable final state of composite fermion (6.8) decay is expected to be four jets formed by four quarks, which was already discussed in refs. [20, 21].

These discussions can be generalized to the decay channels whose intermediate state is a composite quarkonium state $S^{0\pm}$, instead of a composite meson state $\Pi^{0\pm}$, see eqs. (5.6) and (5.7). Also, these discussion can be generalized to the second and third families of composite fermions.

To end this section, we mention other possible channels of composite fermion decay. Analogously to composite-fermion decay channel (6.8), the composite fermions (4.6) formed the quark-lepton interaction decay via the intermediate meson state $\Pi^{\pm}$ (5.39)

$$\Psi_D \to \Pi^+ + [\bar{\nu}_L, \ell_R], \tag{6.9}$$

and its charge conjugate. The final states are a lepton pair and a jet pair. As for the decay of leptonic composite fermions (4.5), final states are: (i) two gauge bosons and a lepton for the neutral channel via the intermediate Π^0 state; (ii) four leptons for the charged channel via the intermediate $\Pi^{\pm}$ state. However these decay rates are much smaller due to the "missing" of the factor N_c^2 and the smallness of the fine-structure constant α relating to the production of leptons in the LHC pp collision.

6.2 Annihilation of two composite fermions

We turn to qualitative discussions of two composite fermions annihilation into two SM gauge bosons G and G', which should be less measurable process compared with a composite fermion decay, in the experimental view of producing two massive composite fermions and detecting final states. Analogously to the annihilation of electron and positron into two photons in the QED, a composite Dirac fermion and its antiparticle annihilates to two photons, and other massive gauge bosons, see figure 6,

$$\Psi_D + \Psi_D^c \to \gamma\gamma, \gamma Z^0, W^+ W^-, Z^0 Z^0, \cdots \tag{6.10}$$

where the composite Dirac fermion Ψ_D has an electric charge $Q = (2/3, -1/3, -1)$ and mass M_F. Apart from the diphoton final state, the final states of energetic dibosons $W^+ W^-$ and $Z^0 Z^0$ are two "fat" jets in opposite directions, each of them is made by two energetic quarks, or these two bosons can decay into the final states of two lepton pairs. While in the channel $\Psi_D + \Psi_D^c \to \gamma Z^0$, the final states are an energetic photon and a "fat" jet or an energetic photon and a lepton pair.
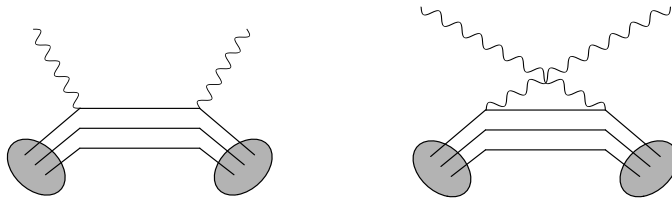
Figure 6. These diagrams show the annihilation of two composite fermions (three solid lines) into two SM gauge bosons (two wave lines).

Given by the mass-energy of two annihilating composite Dirac fermions, the kinematic mass-energy of final states must be larger than $2M_F$. This is not an invariant energy-mass representing the resonance of an unstable composite particle. Suppose that massive composite Dirac fermions produced by the LHC *pp*-collision at present energies are non-relativistic particles,

$$E_F = (|\mathbf{p}_F|^2 + M_F^2)^{1/2} \approx M_F + |\mathbf{p}_F|^2/(2M_F), \tag{6.11}$$

assuming the mass M_F is large enough. Two SM gauge bosons G and G' in the final state (6.10) are ultra-relativistic, the cross-section σ_D of annihilating channel (6.10) can be approximately estimated by using the Dirac rate of point-like electron and positron annihilating to two photons with the replacement $m_e \to M_F$ and $\alpha \to Q^2\alpha$,

$$\sigma_D \sim \pi r_0^2/v, \quad r_0 = Q^2\alpha/M_F, \quad v = |\mathbf{p}_F|/M_F \ll 1, \tag{6.12}$$

up to the form-factors $Z_{L,R}^S$ (4.2) of composite Dirac fermions. The annihilation rate Γ_D per unit time

$$\Gamma_{\Psi_D \Psi_D^c \to \gamma\gamma} \approx \sigma_D v n \sim 2\pi r_0^2 n \sim (Q^2\alpha)^2 M_F \tag{6.13}$$

where the number density of the produced composite fermions $n \sim M_F^3/\pi$ is assumed. Analogously to the positronium state of electron and positron pair in the QED, it is possible that the composite fermion and its antiparticle form an intermediate unstable Coulomb bound state, then decaying into photons or other massive gauge bosons. The spin singlet of the bound state decays into two photons (even number of photons) with the probability $\sim (Q^2\alpha)^5 M_F$, The spin triplet of the bound state decays into three photons (odd number of photons) with the probability $\sim (Q^2\alpha)^6 M_F$. In these discussions, we adopt two-photon final state. As for other channels of two SM gauge bosons G and G' (6.10), in terms of their SM gauge couplings in the effective Lagrangian (4.8), we can obtain the ratios of different annihilation processes:

$$\Gamma_{\Psi_D \Psi_D^c \to \gamma Z^0}/\Gamma_{\Psi_D \Psi_D^c \to \gamma\gamma}, \quad \Gamma_{\Psi_D \Psi_D^c \to W^+ W^-}/\Gamma_{\Psi_D \Psi_D^c \to \gamma\gamma}, \quad \Gamma_{\Psi_D \Psi_D^c \to Z^0 Z^0}/\Gamma_{\Psi_D \Psi_D^c \to \gamma\gamma}, \tag{6.14}$$

depending only on the SM gauge couplings g and g' (4.8) at the mass scale M_F, similarly to the ratios (5.38).

The following annihilation channels of two composite fermions with different charges or zero charge are also possible,

$$\Psi_D^{-1/3} + \Psi_D^{c2/3} \to W^-\gamma, W^- Z^0, \cdots$$
$$\Psi_D^0 + \Psi_D^0 \to W^+ W^-, Z^0 Z^0, \cdots \tag{6.15}$$

and their charged conjugates. In addition, it is known that the annihilation of electron and positron, through an intermediate γ-photon or Z^0-boson, produce a pair of particle and antiparticle in the SM. Analogously, a composite fermion and its antiparticle annihilates, through an intermediate photon or Z^0-boson, and produce a pair of SM elementary particle and its antiparticle,

$$\Psi_D + \Psi_D^c \rightarrow f + f^c, \tag{6.16}$$

where the final state is an energetic lepton pair or quark pair, the former is the dilepton channel and the latter is the dijet channel. Similarly to the channels (6.15) two composite Dirac fermions with different charges or zero charge can annihilate, through an intermediate charged boson $W^\pm$ or neutral boson Z^0, to the pair of two SM elementary fermions.

The analogous discussions on these possible processes can be also made for the case of the composite fermion Ψ_S (singlet) coupling to the γ and Z^0, see eq. (4.8); as well as for the case of composite bosons $\mathcal{A}^i$ coupling to the γ, Z^0 and $W^\pm$, see eq. (4.9). In the effective Lagrangian (4.8) and (4.9), we neglect the interactions between the composite particles, e.g., the composite fermion and boson interaction of the Yukawa type. Thus we skip the discussions on two composite Dirac fermions annihilate to two composite bosons $\mathcal{A}$ and $\mathcal{A}^\dagger$. Limited by the lengthy of this article, it is impossible to discuss even qualitatively all possible processes of the effective Lagrangian (4.8) and (4.9), thus we are led to some considerations and speculations possibly relevant to experiments and /or observations.

7   Some speculative considerations for experiments

In this article, for readers' convenience, we first give a very brief review of effective four-fermion operators and effective theories of elementary and composite particles in IR and UV scaling domains. We then focus the discussions on the decay and annihilation channels of composite bosons and fermions into the final states of the SM gauge bosons, leptons and quarks, in connection with the searches of high-energy experiments, like the ATLAS and CMS. The possibilities and possible criteria are provided for the verification or falsification of such an effective theory of massive composite particles and SM gauge couplings in the UV-domain of strong four-fermion couplings. Obviously, in addition to those processes discussed in this article, there are other possible experimentally relevant processes of effective four-fermion operators (2.6), we end this lengthy article by making some speculative considerations for experiments.

7.1   Some speculative considerations for LHC experiments

In the LHC pp collisions, the most probably channels of producing composite particles are the composite bosons and fermions (4.1)–(4.4) in the first family via the four-fermion operators [20, 21]

$$G\left[(\bar{\psi}_L^{ia} u_{Ra})(\bar{u}_R^b \psi_{Lb}^i) + (\bar{\psi}_L^{ia} d_{Ra})(\bar{d}_R^b \psi_{Lb}^i)\right] + G(\bar{\psi}_L^{ia}\nu_R)(\bar{\nu}_R\psi_L^{ia}), \tag{7.1}$$

and the channels of producing composite particles by other quark and lepton families have smaller rate because of involving small SM gauge interactions. The last term of eq. (7.1)

represents the interaction of quarks and dark-matter particle ν_R, which stands for the right-handed sterile neutrino of the first fermion family.

These composite bosons and fermions could be experimentally verified by possibly observing their resonances and measuring their invariant masses ($\mathcal{M}_{\rm inv}$) and kinematic distributions of relevant final states. If the CM energy $\sqrt{s}$ of LHC pp-collisions is close to the masses M_{Π^0} and M_F of composite boson and fermion ($\sqrt{s} \gtrsim M_{\Pi^0}, M_F$), then the invariant mass $\mathcal{M}_{\rm inv} \sim M_{\Pi^0}$ or $\mathcal{M}_{\rm inv} \sim M_F$. The mass scales M_{Π^0} and M_F can only be determined by high-energy experiments, though we have the theoretical relation $M_F > M_\Pi \propto \mathcal{E}_\xi$ of eq. (4.12) and preliminary theoretical estimation (3.19) on the characteristic energy scale $\mathcal{E}_\xi \gtrsim 5\,{\rm TeV}$ of the UV-domain.

Suppose that the recent ATLAS and CMS preliminary results [69, 70] of diboson resonances (dijets tagged by two bosons) with invariant masses in the energy range from 1.3 to 3.0 TeV could be further confirmed. These resonances are expected to be also seen in the channels of four quark jets, whose invariant mass and event rate should be larger, provided that these resonances are attributed to massive composite Dirac fermions at this energy range. The CMS result [71] of resonances with final states being two jets could include the event of four quark jets, two of them are geometrically close together to form a "wide jet", which should be tagged through a study of its substructure and flavor. Moreover, if composite Dirac fermions are formed by the last operator in eq. (7.1), in addition to jets in final state, dark-matter particles ν_R carry away missing energy-momentum [72, 73]. Similar discussions are applied for the case of composite bosons.

Due to the $W^{\pm}$- and Z^0-boson couplings g_2 to two constituent quarks (u, d) of composite fermions, in particular $W^{\pm}$-boson coupling to $SU_L(2)$ doublet $\psi_L^{ia} = (u_L^a, d_L^a)$, massive composite Dirac fermions have the following decay channels of final states: (i) dijets tagged by two highly boosted bosons WW, WZ or ZZ produced by high-energy constituent quarks (u, d) of composite fermions, together with additional quark jets; (ii) four quark jets formed by four high-energy constituent quarks (u, d) of a composite fermion with a peculiar kinematic distribution [20, 21]. It is expected that the former should have smaller rate because of the SM gauge coupling g_2, although we have not yet been able to calculate the rates of these channels. In these two aforementioned channels (i) and (ii), the final states can also be high-energy leptons, however the branching ratio of $W^{\pm}$ and Z^0 decaying into leptons is about several times smaller than that to hadrons (jets) [67]. The composite fermion can also decay in the channel of W and Higgs (WH) bosons [68], where the Higgs boson is produced by u, d-quarks fusing into a top-quark pair via a gluon, and its production rate is then related to the QCD coupling $\alpha_s = g_3^2/4\pi$. Similar discussions are applied for the case of composite bosons.

7.2 Sterile neutrinos interacting with SM particles at high energies

Last but not least, all sterile neutrinos (ν_R^i, ν_R^{ic}) and SM gauge-singlet (neutral) states of massive composite fermions, e.g., $\boldsymbol{\Psi}_D \sim [\bar\nu_R^\ell, (\bar\ell_L^i \nu_R^\ell)\ell_{Li}]$, can be possible candidates of warm and cold dark matter [19, 21]. They can couple or decay into the SM elementary particles in the following ways. (i) SM gauge-singlet (neutral) states of composite Dirac fermions become unstable and decay into SM elementary particles. (ii) Sterile neutrinos interact

with SM elementary particles via the last term of eq. (7.1) for ψ_L^i being quark or lepton $SU_L(2)$-doublets. (iii) The terms in eqs. (2.16) and (2.17) give the interactions

$$G\left[(\bar{\ell}_L^i \nu_R^\ell)(\bar{\nu}_R^\ell \ell_{Li}) + (\bar{\nu}_R^{\ell c} \ell_R)(\bar{\ell}_R \nu_R^{\ell c}) + (\bar{\nu}_R^{\ell c} u_{a,R}^\ell)(\bar{u}_{a,R}^\ell \nu_R^{\ell c}) + (\bar{\nu}_R^{\ell c} d_{a,R}^\ell)(\bar{d}_{a,R}^\ell \nu_R^{\ell c})\right], \quad (7.2)$$

among sterile neutrinos $\nu_R^\ell, \nu_R^{\ell c}$ (dark matter) and SM elementary particles, where the lepton $SU_L(2)$ doublets $\ell_L^i = (\nu_L^\ell, \ell_L)$, singlets ℓ_R and the conjugate fields of sterile neutrinos $\nu_R^{\ell c} = i\gamma_2(\nu_R^\ell)^*$ ($\ell = e, \mu, \tau$), and quark fields $u_{a,R}^\ell = (u, c, t)_{a,R}$ and $d_{a,R}^\ell = (d, s, b)_{a,R}$.

The four-fermion coupling G in eqs. (7.1) and (7.2) is unique. Therefore, it is expected that at the same energy scale $M_F > M_\Pi \propto \mathcal{E}_\xi$ (4.12), at which composite boson and fermion (4.1)–(4.4) appear as resonances in the LHC pp collisions, leptonic composite boson $(\bar{e}_R \nu_R^{ec})$ or $(\bar{\nu}_R^e e_L)$ and composite fermion $[\bar{\nu}_R^{ec}, (\bar{e}_R \nu_R^{ec})e_R]$ or $[\bar{e}_L, (\bar{\nu}_R^e e_L)\nu_R^e]$ should be formed by high-energy sterile neutrino inelastic collisions, e.g. $\nu_R^e + \bar{\nu}_R^e \rightarrow e^- + e^+$ via the first or second interaction in eq. (7.2). Then these leptonic composite particles decay and produce electrons and positrons. This may account for an excess of cosmic ray electrons and positrons around TeV scale [74–77] in space laboratories. In addition, recent AMS-02 results [78] show that at TeV scale the energy-dependent proton flux changes its power-law index. This implies that there would be "excess" TeV protons whose origin could be also explained by the resonance of composite bosons and fermions due to the interactions (7.1) and (7.2) of dark-matter and normal-matter particles.

We also expect that at the same energy scale $M_F > M_\Pi \propto \mathcal{E}_\xi$ (4.12), the four-fermion interactions of the last term in eq. (7.1), the third and fourth terms in eq. (7.2) form composite fermions made by u, d-quarks and sterile neutrino ν_R, e.g., $[\bar{\psi}_{La}^i, (\bar{\nu}_R \psi_{La}^i)\nu_R]$, $[\bar{\nu}_R^{\ell c}, (\bar{u}_{aR} \nu_R^{\ell c})u_{aR}]$ or $[\bar{u}_{aL}, (\bar{\nu}_R^\ell u_{aL})\nu_R^\ell]$. These composite states should appear as resonances by high-energy sterile neutrinos inelastic collisions with nucleons (xenon) at the largest cross-section, then resonances decay and produce some other detectable SM particles in underground laboratories [79]. Similarly, in the ICECUBE experiment [80], we expect the events that neutrinos change (lose) their directions (energies) by the first term of the interaction (2.16) to form the resonances of composite bosons and fermions at the same energy scale $M_F > M_\Pi \propto \mathcal{E}_\xi$ (4.12). In these inelastic collisions, if the accessible CM energy $\sqrt{s} > M_{\Pi,F}$, the cross section for the allowed inelastic processes forming massive composite bosons and fermions will be geometrical in magnitude, of order $\sigma_{\text{com}} \sim 4\pi/M_{\Pi,F}^2$ in the CM frame where massive composite bosons and fermions are approximately at rest.

7.3 Further studies

By contrast with the low-energy effective theory of SM elementary particles in the IR-domain of weak four-fermion coupling, we have to confess that the present analysis of the effective theory of composite particles in the UV-domain of strong four-fermion coupling are completely preliminary, due to its non-perturbative nature from the theoretical point view. Adequate non-perturbative methods both analytical approaches and numerical algorithms are necessary. This is analogous to the theoretical aspects of low-energy hadron physics of non-perturbative QCD. On the other hand, from experimental point of view, it is nontrivial to proceed physically sensible final-state selection and relevant data analysis in high-energy

experiments, in addition to searching for high-energy collisions and accumulating enough data for significant analysis. However, without high-energy experiments, the characteristic energy scale $M_F > M_\Pi \propto \mathcal{E}_\xi$ (4.12) of effective composite-particle theory cannot even be determined at all. It is worthwhile to mention that similar to the analogy between the Higgs mechanism and Bardeen-Cooper-Schrieffer (BCS) superconductivity, we are studying an analogy between the effective theory discussed in this article and the BCS-BEC (Bose-Einstein condensate) crossover and unitary Fermi gas of strong-interacting electrons [81], which is expected to observe in optical lattice.

Acknowledgments

References

[1] Y. Nambu and G. Jona-Lasinio, *Dynamical Model of Elementary Particles Based on an Analogy with Superconductivity. 1.*, *Phys. Rev.* **122** (1961) 345 [INSPIRE].

[2] F. Englert and R. Brout, *Broken Symmetry and the Mass of Gauge Vector Mesons*, *Phys. Rev. Lett.* **13** (1964) 321 [INSPIRE].

[3] P.W. Higgs, *Broken symmetries, massless particles and gauge fields*, *Phys. Lett.* **12** (1964) 132 [INSPIRE].

[4] P.W. Higgs, *Broken Symmetries and the Masses of Gauge Bosons*, *Phys. Rev. Lett.* **13** (1964) 508 [INSPIRE].

[5] P.W. Higgs, *Spontaneous Symmetry Breakdown without Massless Bosons*, *Phys. Rev.* **145** (1966) 1156 [INSPIRE].

[6] G.S. Guralnik, C.R. Hagen and T.W.B. Kibble, *Global Conservation Laws and Massless Particles*, *Phys. Rev. Lett.* **13** (1964) 585 [INSPIRE].

[7] T.W.B. Kibble, *Symmetry breaking in nonAbelian gauge theories*, *Phys. Rev.* **155** (1967) 1554 [INSPIRE].

[8] ATLAS collaboration, *Observation of a new particle in the search for the Standard Model Higgs boson with the ATLAS detector at the LHC*, *Phys. Lett.* **B 716** (2012) 1 [arXiv:1207.7214] [INSPIRE].

[9] CMS collaboration, *Observation of a new boson at a mass of 125 GeV with the CMS experiment at the LHC*, *Phys. Lett.* **B 716** (2012) 30 [arXiv:1207.7235] [INSPIRE].

[10] ATLAS collaboration, *Search for resonances in diphoton events at $\sqrt{s} = 13\,TeV$ with the ATLAS detector*, *JHEP* **09** (2016) 001 [arXiv:1606.03833] [INSPIRE].

[11] CMS collaboration, *Search for Resonant Production of High-Mass Photon Pairs in Proton-Proton Collisions at $\sqrt{s} = 8$ and 13 TeV*, *Phys. Rev. Lett.* **117** (2016) 051802 [arXiv:1606.04093] [INSPIRE].

[12] S.-S. Xue, *Vectorlike $W^{\pm}$-boson coupling at TeV and third family fermion masses*, *Phys. Rev.* **D 93** (2016) 073001 [arXiv:1506.05994] [INSPIRE].

[13] S.-S. Xue, *Hierarchy spectrum of SM fermions: from top quark to electron neutrino*, *JHEP* **11** (2016) 072 [arXiv:1605.01266] [INSPIRE].

[14] S.-S. Xue, *A lattice chiral theory with multi-fermion couplings*, *Phys. Lett.* **B 381** (1996) 277 [hep-lat/9605003] [INSPIRE].

[15] S.-S. Xue, *A possible scaling region of chiral fermions on a lattice*, *Nucl. Phys.* **B 486** (1997) 282 [hep-lat/9605005] [INSPIRE].

[16] S.-S. Xue, *Chiral gauged fermions on a lattice*, *Nucl. Phys.* **B 580** (2000) 365 [hep-lat/0002026] [INSPIRE].

[17] S.-S. Xue, *A further study of the possible scaling region of lattice chiral fermions*, *Phys. Rev.* **D 61** (2000) 054502 [hep-lat/9910013] [INSPIRE].

[18] S.-S. Xue, *The (11112) model on a (H1)-dimensional lattice*, *Phys. Rev.* **D 64** (2001) 094504 [hep-lat/0109002] [INSPIRE].

[19] S.-S. Xue, *On the standard model and parity conservation*, *J. Phys.* **G 29** (2003) 2381 [INSPIRE].

[20] S.-S. Xue, *Ultraviolet fixed point and massive composite particles in TeV scales*, *Phys. Lett.* **B 737** (2014) 172 [arXiv:1405.1867] [INSPIRE].

[21] S.-S. Xue, *Resonant and nonresonant new phenomena of four-fermion operators for experimental searches*, *Phys. Lett.* **B 744** (2015) 88 [arXiv:1501.06844] [INSPIRE].

[22] C.T. Hill, *Topcolor: Top quark condensation in a gauge extension of the standard model*, *Phys. Lett.* **B 266** (1991) 419 [INSPIRE].

[23] C.T. Hill, *Topcolor assisted technicolor*, *Phys. Lett.* **B 345** (1995) 483 [hep-ph/9411426] [INSPIRE].

[24] C.T. Hill, *'Super'-Dilatation Symmetry of the Top-Higgs System*, *Phys. Rev.* **D 87** (2013) 065002 [arXiv:1211.2773] [INSPIRE].

[25] C.T. Hill, *Quark and Lepton Masses from Renormalization Group Fixed Points*, *Phys. Rev.* **D 24** (1981) 691 [INSPIRE].

[26] C.T. Hill, C.N. Leung and S. Rao, *Renormalization Group Fixed Points and the Higgs Boson Spectrum*, *Nucl. Phys.* **B 262** (1985) 517 [INSPIRE].

[27] J. Bagger, S. Dimopoulos and E. Masso, *Renormalization Group Constraints in Supersymmetric Theories*, *Phys. Rev. Lett.* **55** (1985) 920 [INSPIRE].

[28] W.A. Bardeen, C.T. Hill and M. Lindner, *Minimal Dynamical Symmetry Breaking of the Standard Model*, *Phys. Rev.* **D 41** (1990) 1647 [INSPIRE].

[29] Y. Nambu, *Model Building Based on Bootstrap Symmetry Breaking, in Proceedings of the 1989 workshop on Dynamical Symmetry Breaking*, in proceedings of the *1989 Workshop on Dynamical Symmetry Breaking*, T. Muta and K. Yamawaki eds., Nagoya University, Nagoya, Japan (1990).

[30] V.A. Miransky, M. Tanabashi and K. Yamawaki, *Is the t Quark Responsible for the Mass of W and Z Bosons?*, *Mod. Phys. Lett.* **A 4** (1989) 1043 [ɪɴSPIRE].

[31] V.A. Miransky, M. Tanabashi and K. Yamawaki, *Dynamical electroweak symmetry breaking with large anomalous dimension and t quark condensate*, *Phys. Lett.* **B 221** (1989) 117.

[32] H. Kleinert, *Particles an Quantum Field*, Chapter 26, World Scientific Publishing Company, (2016), http://klnrt.de/b6.

[33] W.J. Marciano, *Heavy top quark mass predictions*, *Phys. Rev. Lett.* **62** (1989) 2793 [ɪɴSPIRE].

[34] G. Cvetič, *Top quark condensation*, *Rev. Mod. Phys.* **71** (1999) 513 [hep-ph/9702381] [ɪɴSPIRE].

[35] C.T. Hill and E.H. Simmons, *Strong dynamics and electroweak symmetry breaking*, *Phys. Rept.* **381** (2003) 235 [*Erratum ibid.* **390** (2004) 553] [hep-ph/0203079] [ɪɴSPIRE].

[36] S.-S. Xue, *Quantum Regge calculus of Einstein-Cartan theory*, *Phys. Lett.* **B 682** (2009) 300 [arXiv:0902.3407] [ɪɴSPIRE].

[37] S.-S. Xue, *Detailed discussions and calculations of quantum Regge calculus of Einstein-Cartan theory*, *Phys. Rev.* **D 82** (2010) 064039 [arXiv:0912.2435] [ɪɴSPIRE].

[38] S.-S. Xue, *The phase structure of Einstein-Cardan theory*, *Phys. Lett.* **B 665** (2008) 54 [arXiv:0804.4619] [ɪɴSPIRE].

[39] S.-S. Xue, *The Phase and Critical Point of Quantum Einstein-Cartan Gravity*, *Phys. Lett.* **B 711** (2012) 404 [arXiv:1112.1323] [ɪɴSPIRE].

[40] H.B. Nielsen and M. Ninomiya, *Absence of Neutrinos on a Lattice. 1. Proof by Homotopy Theory*, *Nucl. Phys.* **B 185** (1981) 20 [*Erratum ibid.* **B 195** (1982) 541] [ɪɴSPIRE].

[41] H.B. Nielsen and M. Ninomiya, *No Go Theorem for Regularizing Chiral Fermions*, *Phys. Lett.* **B 105** (1981) 219 [ɪɴSPIRE].

[42] H.B. Nielsen and M. Ninomiya, *Intuitive understanding of anomalies: A Paradox with regularization*, *Int. J. Mod. Phys.* **A 6** (1991) 2913 [ɪɴSPIRE].

[43] H. Kleinert, *On the hadronization of quark theories*, in *Understanding the fundamental constituents of matter*, A. Zichichi ed., Plenum Press, New York U.S.A. (1978).

[44] C. Itzykson and J-B. Zuber, *Quantum Feild Theory*, pg. 161, McGraw-Hill, Inc. ISBN 0-07-032071-3.

[45] T.P. Cheng and L.F. Li, *Gauge theory of elementary particle physics*, Oxford University Press Inc., New York, U.S.A. (1984), ISBN 978-019-851961-4.

[46] R.N. Mohapatra and P.B. Pal, *Massive Neutrinos in Physics and Astro-physics*, third edition, World Scientific, (2004).

[47] S.-S. Xue, *Neutrino masses and mixings*, *Mod. Phys. Lett.* **A 14** (1999) 2701 [hep-ph/9706301] [ɪɴSPIRE].

[48] E. Eichten and J. Preskill, *Chiral Gauge Theories on the Lattice*, *Nucl. Phys.* **B 268** (1986) 179 [ɪɴSPIRE].

[49] M. Creutz, M. Tytgat, C. Rebbi and S.-S. Xue, *Lattice formulation of the standard model*, *Phys. Lett.* **B 402** (1997) 341 [hep-lat/9612017] [ɪɴSPIRE].

[50] S.-S. Xue, *Why is the top quark much heavier than other fermions?*, *Phys. Lett.* **B 721** (2013) 347 [`arXiv:1301.4254`] [INSPIRE].

[51] S.-S. Xue, *Higgs Boson and Top-Quark Masses and Parity-Symmetry Restoration*, *Phys. Lett.* **B 727** (2013) 308 [`arXiv:1308.6486`] [INSPIRE].

[52] ATLAS collaboration, *Search for contact interactions and large extra dimensions in dilepton events from pp collisions at $\sqrt{s} = 7$ TeV with the ATLAS detector*, *Phys. Rev.* **D 87** (2013) 015010 [`arXiv:1211.1150`] [INSPIRE].

[53] D. Bai, J.-W. Cui and Y.-L. Wu, *Quantum Electroweak Symmetry Breaking Through Loop Quadratic Contributions*, *Phys. Lett.* **B 746** (2015) 379 [`arXiv:1412.3562`] [INSPIRE].

[54] M. Gell-Mann and M. Lèvy, *The axial vector current in beta decay*, *Nuovo Cim.* **16** (1960) 705 [INSPIRE].

[55] J. Zinn-Justin, *Quantum Field Theory and Critical Phenomena*, Oxford University Press, (2002).

[56] J.L. Cardy, *Scaling and the Renormalization Group in Statistical Physics*, Cambridge University Press, (1997).

[57] E. Brézin and J. Zinn-Justin, *Renormalization of the nonlinear σ-model in $2 + \epsilon$ dimensions — Application to the Heisenberg ferromagnets*, *Phys. Rev. Lett.* **36** (1976) 691 [INSPIRE].

[58] H. Kleinert, *Particles and Quantum Field*, World Scientific Publishing Company, (2016).

[59] S. Weinberg, *Elementary particle theory of composite particles*, *Phys. Rev.* **130** (1963) 776 [INSPIRE].

[60] S. Weinberg, *Quasiparticles and the Born Series*, *Phys. Rev.* **131** (1963) 440 [INSPIRE].

[61] S. Weinberg, *Systematic Solution of Multiparticle Scattering Problems*, *Phys. Rev.* **133** (1964) B232 [INSPIRE].

[62] S. Weinberg, *Evidence That the Deuteron Is Not an Elementary Particle*, *Phys. Rev.* **137** (1965) B672 [INSPIRE].

[63] S. Weinberg, *Critical Phenomena for Field Theorists, in Understanding the Fundamental Constituents of Matter*, in *Understanding the Fundamental Constituents of Matter*, A. Zichichi ed., Plenum Press, New York, U.S.A. (1977).

[64] H. Kleinert, *Particles and Quantum Field*, Chapter 30, World Scientific Publishing Company, (2016), http://klnrt.de/b6.

[65] J. Preskill, *Gauge anomalies in an effective field theory*, *Annals Phys.* **210** (1991) 323 [INSPIRE].

[66] M.E. Peskin and D.V. Schroeder, *An Introduction to Quantum Field Theory*, Westview Press, (1995), ISBN-13 978-0-201-50397-5.

[67] PARTICLE DATA GROUP collaboration, J. Beringer et al., *Review of Particle Physics (RPP)*, *Phys. Rev.* **D 86** (2012) 010001 [INSPIRE].

[68] CMS collaboration, *Search for massive WH resonances decaying to $\ell\nu b\bar{b}$ final state in the boosted regime at $\sqrt{s} = 8$ TeV*, CMS-PAS-EXO-14-010 (2014).

[69] ATLAS collaboration, *Search for high-mass diboson resonances with boson-tagged jets in proton-proton collisions at $\sqrt{s} = 8$ TeV with the ATLAS detector*, *JHEP* **12** (2015) 055 [`arXiv:1506.00962`] [INSPIRE].

[70] CMS collaboration, *Search for resonances and quantum black holes using dijet mass spectra in proton-proton collisions at* $\sqrt{s} = 8\,TeV$, *Phys. Rev.* **D 91** (2015) 052009 [arXiv:1501.04198] [INSPIRE].

[71] CMS collaboration, *Search for massive resonances in dijet systems containing jets tagged as W or Z boson decays in pp collisions at* $\sqrt{s} = 8\,TeV$, *JHEP* **08** (2014) 173 [arXiv:1405.1994] [INSPIRE].

[72] ATLAS collaboration, *Search for Dark Matter in Events with Missing Transverse Momentum and a Higgs Boson Decaying to Two Photons in pp Collisions at* $\sqrt{s} = 8\,TeV$ *with the ATLAS Detector*, *Phys. Rev. Lett.* **115** (2015) 131801 [arXiv:1506.01081] [INSPIRE].

[73] CMS collaboration, *Search for the production of dark matter in association with top-quark pairs in the single-lepton final state in proton-proton collisions at* $\sqrt{s} = 8\,TeV$, *JHEP* **06** (2015) 121 [arXiv:1504.03198] [INSPIRE].

[74] J. Chang et al., *An excess of cosmic ray electrons at energies of 300–800 GeV*, *Nature* **456** (2008) 362 [INSPIRE].

[75] Y.-Z. Fan, B. Zhang and J. Chang, $e^{\pm}$ *Excesses in the Cosmic Ray Spectrum and Possible Interpretations*, *Int. J. Mod. Phys.* **D 19** (2010) 2011 [arXiv:1008.4646] [INSPIRE].

[76] N. Arkani-Hamed, D.P. Finkbeiner, T.R. Slatyer and N. Weiner, *A Theory of Dark Matter*, *Phys. Rev.* **D 79** (2009) 015014 [arXiv:0810.0713] [INSPIRE].

[77] D. Malyshev, I. Cholis and J. Gelfand, *Pulsars versus Dark Matter Interpretation of ATIC/PAMELA*, *Phys. Rev.* **D 80** (2009) 063005 [arXiv:0903.1310] [INSPIRE].

[78] AMS collaboration, M. Aguilar et al., *Precision Measurement of the Proton Flux in Primary Cosmic Rays from Rigidity 1 GV to 1.8 TV with the Alpha Magnetic Spectrometer on the International Space Station*, *Phys. Rev. Lett.* **114** (2015) 171103 [INSPIRE].

[79] http://pandax.physics.sjtu.edu.cn/.

[80] https://icecube.wisc.edu/.

[81] H. Kleinert and S.-S. Xue, *Fermion Bound States in a Strongly-Coupled Fermion Liquid*, in preparation.